

A long-term dataset of simulated epilimnion and hypolimnion temperatures in 401 French lakes (1959-2020)

Najwa Sharaf^{1,2}, Jordi Prats³, Nathalie Reynaud^{1,2}, Thierry Tormos^{1,4}, Rosalie Bruel^{1,4},
Tiphaine Peroux^{1,2}, Pierre-Alain Danis^{1,4}

¹Pôle R&D Ecosystèmes Lacustres (ECLA), OFB-INRAE-USMB, Aix-en-Provence, France

²INRAE, Aix Marseille Univ, RECOVER, Team FRESHCO, 3275 Route Cézanne, 13182 Aix-en-Provence, France

³Segula-³SEGULA Technologies, C. Calàbria 169, 08015 Barcelona, Spain

⁴OFB, Service ECOAQUA, DRAS, 3275 Route Cézanne, 13100 Aix-en-Provence, France

Correspondence to: Sharaf Najwa (najwa.sharaf@inrae.fr), Bruel Rosalie (rosalie.brue1@ofb.gouv.fr), Tormos Thierry (thierry.tormos@ofb.gouv.fr), Reynaud Nathalie (nathalie.reynaud@inrae.fr)

54 **1. Abstract**

55 Understanding the thermal behavior of lakes is crucial for water quality management. Under climate change, lakes
56 are warming and undergoing alterations in their thermal structure, including surface and deep-water temperatures.
57 These changes require continuous monitoring due to the possible major ecological implications on water quality
58 and lake processes. ~~We combined numerical modelling and satellite thermal data to create~~ ~~with the scarcity of long-~~
59 ~~term in situ water temperature datasets, we present~~ a regional ~~long-term water temperature~~ dataset (LakeTSim:
60 Lake Temperature Simulations) ~~of long-term water temperatures for produced over~~ 401 French lakes ~~in order to~~
61 ~~tackle the scarcity of in situ water temperature.~~ ~~by combining numerical modelling and satellite thermal data.~~ The
62 dataset consists of daily epilimnion and hypolimnion ~~water~~ temperatures for the period 1959-2020 simulated with
63 the semi-empirical OKPLM (Ottosson-Kettle-Prats Lake Model) ~~and the associated uncertainties.~~ ~~We also~~
64 ~~describe this~~ ~~Here, we describe the~~ model and its performance. ~~Additionally, we present~~ ~~We present~~ the uncertainty
65 analysis of simulations with default ~~parameter values~~ (parametrized ~~with satellite thermal data over all lakes and~~
66 ~~in situ measurements as a function of lake characteristics~~) and calibrated ~~parameter values~~ ~~(with in situ temperature~~
67 ~~measurements for each lake)~~ ~~model parameters are presented, along with as well as~~ the ~~sensitivity~~ analysis of the
68 ~~sensitivity of the latter model to parameter values and biases in the input data.~~ Overall, the 90% confidence
69 uncertainty range is largest for hypolimnion temperature simulations with a median of 8.5 °C and 2.32 °C
70 respectively with default and calibrated parameter values. There is less uncertainty associated with epilimnion
71 temperature simulations with a median of 5.42 °C and 1.85 °C, ~~respectively~~ before and after parameter calibration.
72 This dataset ~~will help provide insight into the thermal functioning of French lakes.~~ It provides over six decades of
73 epilimnion and hypolimnion temperature data, crucial for climate change studies at a regional scale. ~~It~~ ~~The dataset~~
74 ~~will help provide insight into the thermal functioning of French lakes and can be used to help also be of great~~
75 ~~advantage for~~ decision-making ~~and~~ by stakeholders.

76 **2. Introduction**

77 Lakes, both natural and artificial (i.e., reservoirs and gravel pits) are sentinels of environmental change and provide
78 important services such as access to drinking water, hydropower production, recreation and fisheries (Adrian et
79 al., 2009). Under climate change and anthropogenic pressures, many lakes are warming and consequently
80 experiencing changes to their biophysicochemical structure and function that are leading to services being
81 compromised (Janssen et al., 2021).

82 In lakes, water temperature is an essential parameter regulating processes such as the functioning of trophic webs,
83 oxygen conditions, the physical structure of the water column as well as the biogeochemistry (Yang et al., 2018).
84 Under warming, historical records and future projections demonstrate that for lakes, alterations in the
85 thermodynamic functioning including warmer temperatures and shifts in mixing regimes already took place and
86 are expected to persist in the future (Shatwell et al., 2019; Woolway and Merchant, 2019). In this context, they are
87 undergoing shorter periods of ice cover and longer, more stable periods of thermal stratification (Woolway et al.,
88 2022). These alterations could have considerable ecological implications for the biological communities (Lind et
89 al., 2022; Havens and Jeppesen, 2018). For instance, worldwide studies have shown that the expansion of toxic
90 cyanobacterial blooms is linked to warming (Griffith and Gobler, 2020). Other responses include species reduced
91 body size (Daufresne et al., 2009), changes in thermal habitat and shifts in species seasonality (Kharouba et al.,
92 2018).

93 ~~For assessing the impact of climate change on lake ecosystems~~ It is thus crucial to closely evaluate water
94 temperature trajectories over the entire water column in space and time when assessing the impact of climate
95 change on lake ecosystems. ~~However, the lack of data coverage, both spatially and temporally, makes it difficult~~
96 to accurately characterize lakes thermal response to climate change and to identify warming trends (Gray et al.,
97 2018). Indeed, long-term datasets of in situ temperatures are usually scarce and mostly limited to large lakes
98 (Layden et al., 2015). Moreover, sampling frequency and temporal coverage of in situ water temperature varies
99 greatly from one lake to the next, from a few years (Sharma et al., 2015) up to decades (Piccolroaz et al., 2020;
100 Rimet et al., 2020). ~~long-term datasets of in situ temperatures are usually scarce and mostly limited to large lakes~~
101 (Layden et al., 2015). ~~Moreover, the sampling of water temperature differs in terms of approach and frequency,~~
102 ~~from decades (Piccolroaz et al., 2020) to a few years (Sharma et al., 2015), thus rendering it challenging to~~
103 ~~investigate warming trends(Gray et al., 2018).~~

104 Due to the difficulties in conventional in situ monitoring, ~~which is~~ often expensive, the coupling of modelling and
105 satellite remote sensing data has become fundamental in the field of limnology (Nouchi et al., 2019). Modelling
106 provides means to interpolate both temporal and spatial gaps. It thereby allows us to acquire information about
107 surface water temperatures, which are globally the focus of lake climate change studies, and deep-water
108 temperatures which are as critical though often disregarded in this context. Several numerical models that vary in
109 complexity exist for conducting water temperature simulations, the most accurate being deterministic or process-
110 based models. Nevertheless, regional or global deterministic modelling efforts over long periods are usually
111 hindered by the lack of sufficiently detailed input data (e.g., meteorological and field data) to run the models (Kim
112 et al., 2021). For practical and operational purposes, simpler models (semi-empirical, statistical or hybrid physical-
113 statistical based models) with less requirements for forcing data, have been mostly applied to assess the impact of
114 climate change on lake ecosystems and study them (Piccolroaz et al., 2020; Toffolon et al., 2014; Sharma et al.,
115 2008). Long-term simulations across a considerable number of lakes are made possible with this type of models,
116 enabling the detection of trends in time series data that are not achievable ~~For conducting long term simulations~~
117 ~~over a considerable number of lakes, this type of models is especially useful for detecting trends in time series,~~
118 ~~which~~ with shorter datasets ~~is not accurately achievable~~(Gray et al., 2018).

119 The performance of numerical models depends highly on the calibration of their parameters as well as on the
120 quality of the input data. Satellite remote sensing is an effective way to monitor surface water temperature on a
121 synoptic scale (Schaeffer et al., 2018; Sharaf et al., 2019) and provide a complementary source of data to in situ
122 measurements for model calibration or validation purposes (Allan et al., 2016; Babbar-Sebens et al., 2013). In
123 particular, thermal infrared sensors onboard the Landsat satellites are very adequate for retrospective analysis of
124 surface water temperature with a spatial resolution adapted for small to medium size lakes and reservoirs at a
125 bimonthly acquisition frequency. Landsat 4 and 5 TM (Thematic Mapper), 7 ETM+ (Enhanced Thematic Mapper)
126 and 8 TIRS (Thermal InfraRed Sensor) provide surface temperature data at spatial resolutions of 120, 60 and 100
127 m respectively. Landsat series records of surface water temperature can be used to validate 3D hydrodynamic
128 models when in situ measurements are scarce (Sharaf et al., 2021) and to spatially assess the quality and suitability
129 of aquatic habitat for biological communities (Halverson et al., 2022). Although, satellite thermal data is limited
130 to the surface, its integration into model calibration could improve the accuracy of simulations over the surface
131 layer and the water column (Javaheri et al., 2016).

132 Here we present on a regional scale, a long-term dataset, LakeTSim (Lake Temperature Simulations), of daily
133 epilimnion and hypolimnion temperature simulations, as well as uncertainties, for the period 1959-2020 over 401
134 French lakes monitored under the Water Framework Directive (WFD) including natural and artificial lakes,
135 reservoirs and gravel pits. We present the OKPLM (Ottosson-Kettle-Prats Lake Model) used to produce water
136 temperature simulations and its performance. Further, we provide the uncertainty analysis of simulations with
137 default (parametrized with satellite thermal data over an entire set of lakes) and calibrated (with in situ temperature
138 measurements for each lake) model parameter values as well as the sensitivity analysis for the latter. ~~The goal of~~
139 ~~publishing this dataset is to provide new insight about surface-epi- and deep-waterhypolimnion temperatures of~~
140 ~~lakes in France especially for those that are not monitored regularly through conventional methods. -This long-~~
141 ~~term dataset is valuable for developing temperature indicators for identifying warming trends, extreme events and~~
142 ~~possible changes in the mixing regime among others. These indicators will contribute to assess the impact of~~
143 ~~climate change on lakes thermal functioning and its influence on the biological community structure and trophic~~
144 ~~webs.~~

145 **3. Data and methodology**

146 3.1. The software suite ALAMODE

147 The simulations, ~~and~~ sensitivity and uncertainty analysis presented in this paper were made using the software
148 suite ALAMODE (A Lake MODElling project). ALAMODE (Danis, 2020) is a software suite developed in
149 Python 3 by the Pôle R&D Ecosystèmes Lacustres (ECLA) and SEGULA Technologies to facilitate the realization
150 of simulations of lakes and the management of related information. It comprises multiple modules and packages
151 designed for lake and tributary modeling, as well as for processing the data necessary to operate these models.
152 These packages include OKPLM (Ottosson-Kettle-Prats Lake Model), CUSPY (Calibration, Uncertainty analysis
153 and Sensitivity analysis in PYthon), TMOD (Temperature MODElling), GLMtools (General Lake Model tools),
154 “tributary”, TINDIC (Temperature INDICators) and ALAPROD (ALAMODE-Production). OKPLM (Prats-
155 Rodríguez and Danis, 2023b) is used to simulate epilimnion and hypolimnion water temperatures in lakes while
156 CUSPY (Prats-Rodríguez and Danis, 2023a) is used for model parameters estimations and conducting uncertainty
157 and sensitivity analyses. TMOD is used for managing the T-MOD database designated to facilitate the realization
158 and consultation of simulations. GLMtools is used to conduct lake hydrodynamic simulations using the one-
159 dimensional hydrodynamic General Lake Model (Hipsey et al., 2019) while “tributary” is used for the estimation
160 of flow and temperature of lake tributaries. The package TINDIC is used for calculating temperature indicators
161 from model simulations. Finally, ALAPROD integrates all the functionalities to produce simulations into a single
162 package: simulation of stream water temperature, of lake hydrodynamics and temperature, and of stream flow rate.
163 It also includes sensitivity and uncertainty analysis features. The functionalities of these packages can be accessed
164 either by using each package separately or by utilizing the ALAPROD package, which depends on the TMOD
165 database and requires access to it.

166 At present, only the ALAMODE packages related to the main functionalities used in this work are publicly
167 available (see Code availability section): the simulation of lake temperatures using the Ottosson-Kettle-Prats
168 Lake Model (Prats & Danis, 2019), implemented in the package OKPLM, and the sensitivity and uncertainty
169 analysis tools in the CUSPY package. We used ALAPROD to access the functionalities of both packages.

3.1.3.2. The OKP Lake Model description

The OKPLM (Ottosson-Kettle-Prats Lake Model) (Prats & Danis, 2019) is a two-layer semi-empirical data model adapted from Kettle et al (2004) for the epilimnion module and Ottosson & Abrahamsson (1998) for the hypolimnion module. ~~It was further modified~~The modifications proposed in Prats & Danis (2019)~~and used to simulate daily epilimnion and hypolimnion temperatures of 401 French lakes. These modifications~~ consisted mainly of simplifying the mixing algorithm used in Ottosson & Abrahamsson (1998) using a basic stability condition, whereas for the epilimnion module a sinusoidal fit to average daily solar radiation was used instead of the theoretical clear-sky radiation. The OKPLM also runs on weekly and monthly frequencies. The regionalization of the parameters of the model mainly depends on the geographical and morphological properties of the lake (maximal ~~um~~ depth, volume, surface area, latitude and altitude). The model requires few meteorological forcing data: solar radiation and air temperature.

The model calculates water temperature as follows:

$$T_{e,i} = A + Bf(T_{a,i}^*) + CS_i \quad (1)$$

where T_e is the epilimnion temperature ($^{\circ}\text{C}$), i is the day number, A , B and C are calibration parameters, S is the solar radiation (W m^{-2}) and $f(*)$ is an exponential smoothing function with $T_{a,i}^*$ defined as:

$$T_{a,i}^* = T_{a,i} - MAAT \quad (2)$$

Where $T_{a,i}$ is air temperature ($^{\circ}\text{C}$) and $MAAT$ is the annual mean air temperature ($^{\circ}\text{C}$). The smoothing function $f(*)$ is such that it gives greater weight to the nearest observations and the weights decrease exponentially. It is defined as:

$$f(T_{a,1}^*) = T_{a,1}^* \quad (3)$$

$$f(T_{a,i}^*) = \alpha T_{a,i}^* + (1 - \alpha)f(T_{a,i-1}^*) \quad (4)$$

where α is the smoothing factor. When $\alpha = 1$ there is no smoothing, while the smoothing increases with the decrease in the value of α .

$$T_{h,i} = A \cdot D + E \cdot g(T_{e,i}) \quad (5)$$

where T_h is the hypolimnion temperature ($^{\circ}\text{C}$), D and E are calibration parameters and $g(T_{e,i})$ is an exponential smoothing as follows:-

$$g(T_{e,1}) = T_{e,1} \quad (6)$$

$$g(T_{e,i}) = \beta T_{e,i} + (1 - \beta)g(T_{e,i-1}) \quad (7)$$

where β is the exponential smoothing factor. As for α , there is no smoothing for $\beta = 1$ and the smoothing increases as β approaches zero.

~~The OKPLM is integrated into a Python 3 package, "ALAPROD" (A LAke MODElling project PRODUCTION) which for the present study was used to simulate epilimnion and hypolimnion water temperatures (Danis, 2020). ALAPROD is part of a software environment called ALAMODE (Danis, 2020). In addition to lake water~~

temperature, this package can also be used to make simulations of stream water temperature, hydrodynamics and stream flow rates. In ALAPROD, this package OKPLM can be run in two modes: the “default” mode where model parameters values for each lake are estimated using the parameterization presented in Prats & Danis (2019), and the “calibrated” mode where model parameters are calibrated individually for each lake by using in situ temperature measurements. The “default” parameterization was obtained by using the individually calibrated parameter values to fit appropriate expressions as a function of the characteristics of lakes. provides expressions of the model parameters as a function of lake characteristics (latitude, altitude, surface, volume, depth). The expressions for epilimnion module parameters were derived using surface temperatures estimated from Landsat infrared data acquired between 1999 and 2016 over French lakes (Prats et al., 2018), while the parameterization of hypolimnion parameters was derived from temperature profile data of 357 lakes. In the epilimnion module model parameter values A , B , C , and α are estimated based on lake characteristics (i.e., latitude, altitude, surface area, volume, and depth). These equations were determined using robust regressions and Landsat infrared data from 1999 to 2016 of French lakes to estimate surface temperatures (Prats et al., 2018). In contrast, for the hypolimnion module, parameter values E and β were derived as a function of lake depth and lake type using temperature profile data from 357 lakes; β can have a value of 1 ($E > 0.95$) or 0.13 ($E \leq 0.95$). The parameter D was assigned a constant value of 0.51.

The parametrization of the OKPLM parameters as presented in Prats & Danis (2019) is as follows:

$$A = 39.9 - 0.484L_{Lat} - 4.52 \times 10^{-3}L_{Alt} - 0.167\ln L_A \quad (8)$$

where L_{Lat} is lake latitude ($^{\circ}$ N), L_{Alt} is lake altitude (m) and L_A is lake surface area (m^2).

$$B = 1.058 - 0.0010L_{Dmax} \quad (9)$$

where L_{Dmax} is lake maximal depth (m).

$$C = 1.12 \times 10^{-3} - 3.62 \times 10^{-6}L_{Alt} \quad (10)$$

$$E = e_1 + \frac{1-e_1}{1+\exp[e_3(e_2-\ln L_D)]} \quad (11)$$

where e_1 , e_2 and e_3 are coefficients with respective values of 0.10, 2.0, -1.8 for natural lakes and 0.49, 1.7, -2.0 for artificial lakes (reservoirs, gravel pits, ponds and quarry lakes) and L_D is lake mean depth (m).

$$\alpha = \exp(0.52 - 3.0 \times 10^{-4}L_{Alt} + 0.25\ln L_A - 0.36\ln L_V) \quad (12)$$

where L_V is lake volume (m^3).

3.2.3.3. Input data

The OKPLM was forced with two sources of meteorological data extracted from the SAFRAN (Système d'Analyse Fournissant des Renseignements Adaptés à la Nivologie) analysis system (Durand et al., 1993) and the S2M (SAFRAN–SURFEX/ISBA–Crocus–MEPRA) meteorological reanalysis (Vernay et al., 2015, 2022).

The SAFRAN system provides meteorological variables at an hourly time step estimated through interpolation and assimilation processes with an 8 km square grid. Average daily data from the nearest grid cell was selected

236 for each study site. The difference in altitude between the study site and the grid cell was accounted for by applying
237 an adiabatic elevation correction on air temperature.

238 The S2M model chain combines the SAFRAN meteorological analysis and the SURFEX/ISBA–Crocus snow
239 cover model including MEPR (Modèle Expert d’Aide à la Prévision du Risque d’Avalanche). It is more adapted
240 to mountainous regions as it has a spatial definition where spatial heterogeneity is taken into consideration. The
241 S2M reanalysis uses a vertical resolution of 300 m and is the result of simulations performed over mountainous
242 zones ~~called~~ referred to as “massifs” and covering the French Alps, Pyrenees and Corsica mountainous regions. In
243 order to use S2M meteorological data over each lake an extraction of certain topographic classes is necessary.
244 These include elevation, aspect and slope, which represent the spatial variability over “massifs”. On average, a
245 massif corresponds to a mountainous region of about 1000 km² over which meteorological conditions are
246 considered homogeneous at a given elevation range. Two types of S2M reanalysis simulations exist for each
247 elevation range, one at flat terrain and the other with 8 aspects at 2 different slope angles. For this study, this
248 information (elevation, slope, aspect) was extracted from a Digital Elevation Model (BD Alti, IGN) for each lake
249 over its drainage basin, combined into zones corresponding to S2M topographic classes. ~~each corresponding~~
250 approximately to an average surface of 1000 km². These massifs represent the spatial variability of processes in
251 mountainous regions. ~~We considered a zero slope and A~~ average daily data ~~was used~~ for each study site.

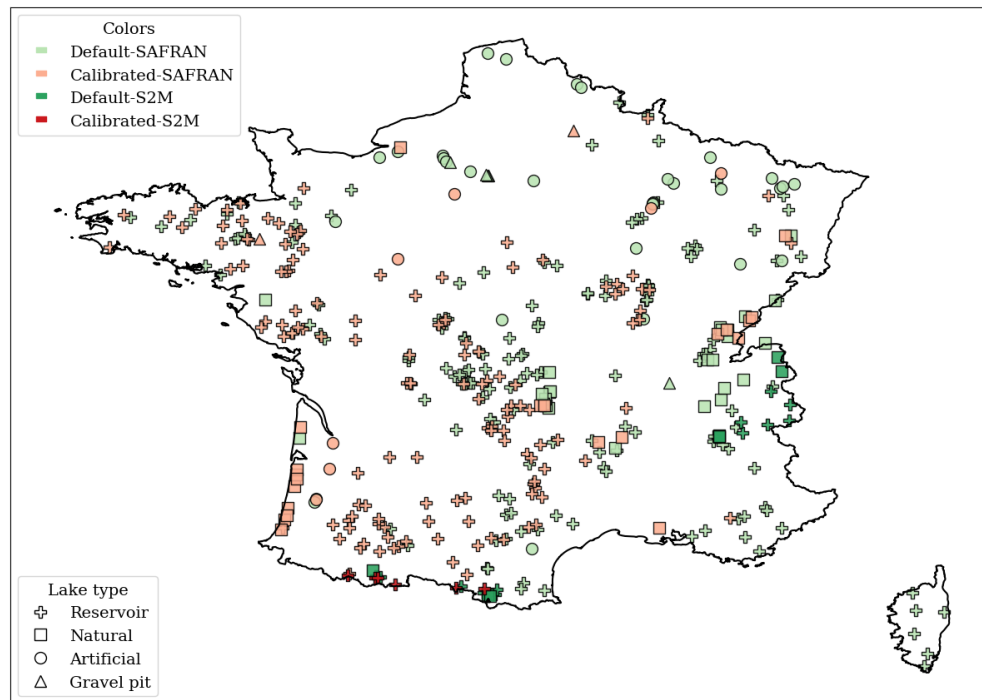
252 In situ temperature profiles, geographical and morphological data of the study sites were initially extracted from
253 the PLAN_DEAU database. The extracted data was then incorporated into the T-MOD database, with the aim of
254 simplifying the process of simulations and accessing information about the characteristics of the simulated lakes.
255 Both databases are managed by INRAE (l’Institut National de Recherche pour l’Agriculture, l’Alimentation et
256 l’Environnement) and Pôle R&D-consortium ECLA (“ECosystèmes Lacustres”) ~~at-in~~ Aix-en-Provence, France.
257 The geomorphological data consisting of maximal depth, volume, surface area, latitude and altitude were extracted
258 for 401 lakes. In situ temperature profiles were extracted for 170 lakes over different depths. Depending on each
259 lake, the number of years with samples could vary from 1 to 12 with a number of samples ranging between 1 and
260 10 per year.

261 3.3.3.4. Lake simulations

262 For this study, we considered 401 lakes (Figure 1) located in Metropolitan France monitored according to the
263 Water Framework Directive (WFD). Here we refer to lakes as natural lakes, reservoirs, ~~artificial lakes and~~ gravel
264 pits and other artificial lakes (e.g., ponds and quarry lakes). The present lake dataset includes epi- and hypolimnion
265 temperature simulations for 54 natural lakes, 302 reservoirs, ~~38 artificial lakes and~~ 7 gravel pits and 38 other
266 artificial lakes (Figure 2). ~~that have~~ The lakes characteristics rangeing between 0 and 2279.7 m for altitude, 0.8
267 and 309.7 m for maximal depth, 0.08 and 577.12 km² for surface area and 5×10^4 and 8.9×10^{10} m³ for volume.

268 The OKPLM was run using “default” and “calibrated” parameters with two sources of meteorological data,
269 “SAFRAN” and “S2M” over specific sets of lakes. “Calibrated” model parameters ~~are~~ were adopted when in situ
270 temperature measurements ~~are~~ were available; conversely, “default” parameters ~~are~~ were used. S2M data are more
271 representative of mountainous meteorological conditions than SAFRAN data and were thus used, when
272 available possible, for simulating the water temperature in lakes situated at altitudes higher than 900 m. For some
273 lakes, it was not possible to use S2M data, either because their drainage basins are not entirely part of a massif (n
274 = 1), or because they are located in massifs that are not covered by the S2M reanalysis dataset ($n = 18$). Among

275 the total number of study sites ($n = 401$), the model was forced using SAFRAN and S2M meteorological data
276 respectively for 210 and 21 lakes with “default” model parameters, and for 164 and 6 lakes with “calibrated” model
277 parameters. ~~The geomorphological characteristics of the simulated lakes with each of the abovementioned~~
278 ~~configurations are shown in Table 1. “Calibrated” model parameters are adopted when in situ temperature~~
279 ~~measurements are available; conversely, “default” parameters are used. S2M data are more representative of~~
280 ~~mountainous meteorological conditions than SAFRAN data and were thus used for simulating the water~~
281 ~~temperature in lakes situated at altitudes higher than 900 m.~~



282

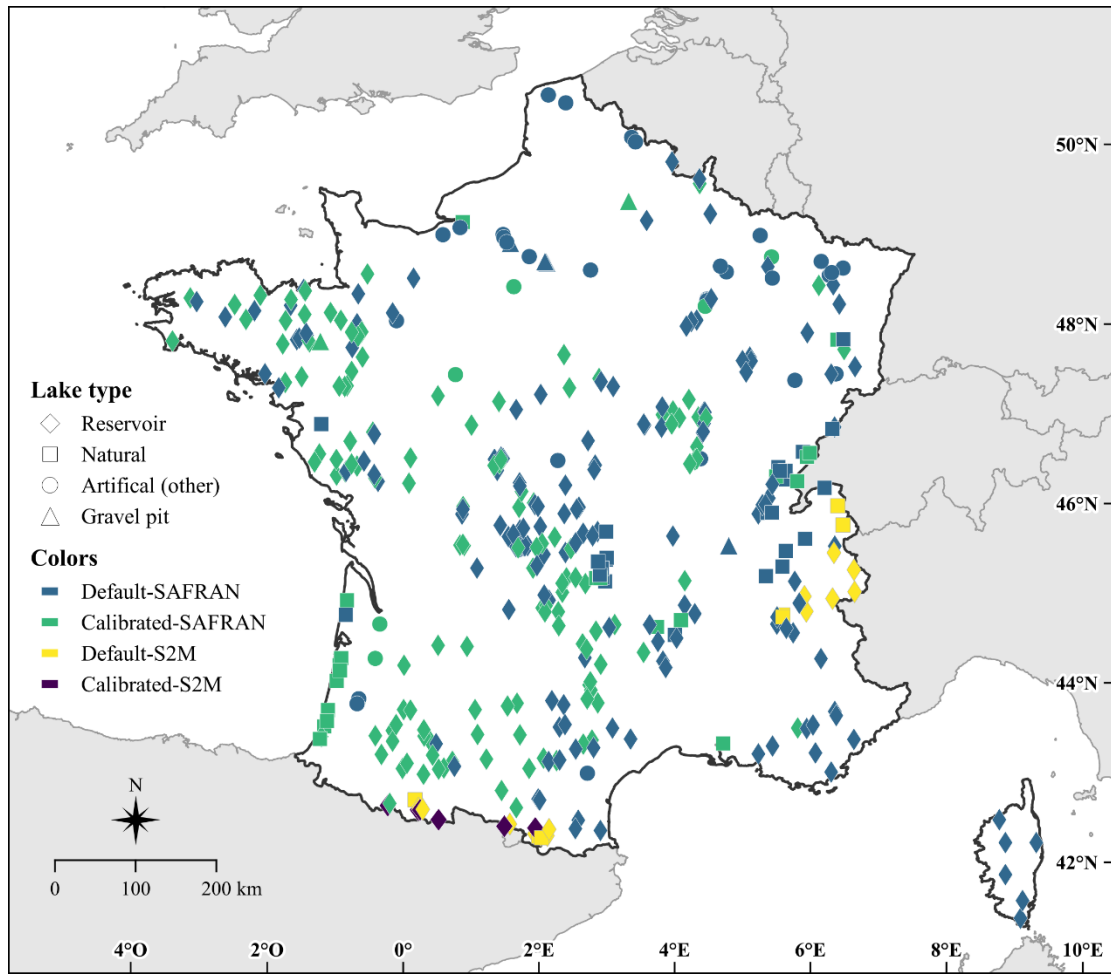


Figure 1: Location and lake type of the 401 French lakes simulated with the OKPLM in “default” and “calibrated” modes, with SAFRAN and S2M meteorological data for the period 1959-2020.

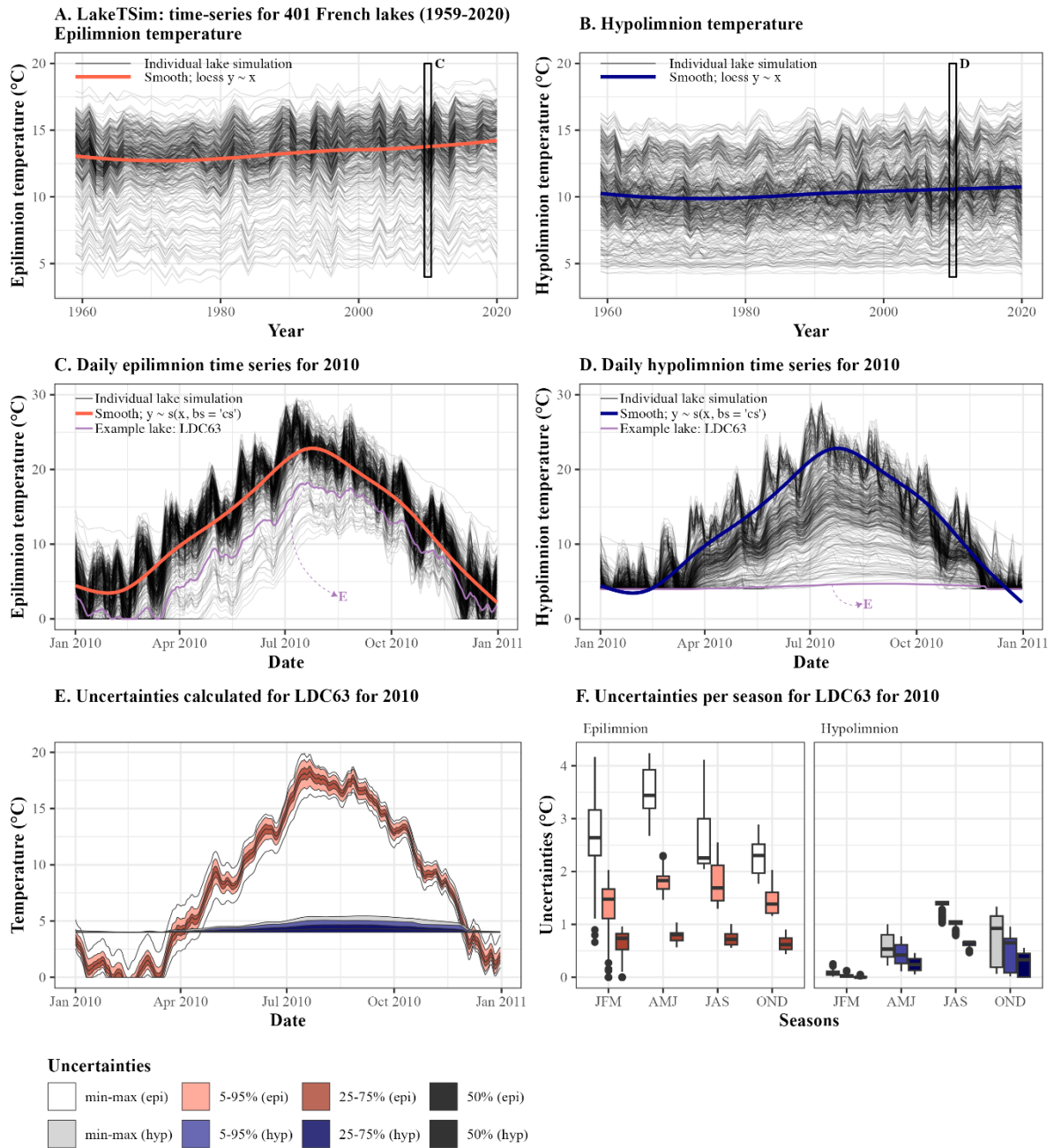


Figure 2: Presentation of the LakeTSim data. (A) Epilimnion and (B) hypolimnion mean annual temperatures, with average trend across lakes shown with a smooth spline. (C) Daily epilimnion temperature per lake in the dataset for 2010, with smooth spline and the time series for one lake (LDC63) highlighted. (D) Daily hypolimnion temperature per lake in the dataset for 2010, with smooth spline and the time series for one lake (LDC63) highlighted. LDC63 is the code for Lake Chauvet, a natural lake (45.46 °N, 2.83 °E) located at 1167 m asl, with a surface area of 0.51 km², a volume of 17.41 10⁶ m³, and a maximum depth of 66.8 m. The simulation for LDC63 was conducted resorting to SAFRAN data and was run with the “calibrated” mode. (E) Uncertainties were calculated per lake and per day and are shown here daily for LDC63, in 2010, for both the epilimnion (epi) and the hypolimnion (hyp). (F) Uncertainties are shown here seasonally for LDC63, in 2010, for both the epilimnion (epi) and the hypolimnion (hyp). JFM corresponds to January-February-March, AMJ corresponds to April-May-June, JAS corresponds to July-August-September and OND corresponds to October-November-December.

Table 1: Characteristics of the lakes simulated with the OKPLM in “default” and “calibrated” modes with SAFRAN and S2M meteorological data for the period 1959-2020; n represents the number of lakes.

Variables	Minimal - Maximal range			
Model parameters	Default		Calibrated	
Meteorological data	SAFRAN	S2M	SAFRAN	S2M
n	210	21	164	6
Altitude (m)	1 - 1753	916 - 2213	0 - 2279.7	1577.5 - 2172.5
Latitude (°N)	41.47 - 50.87	42.55 - 46.21	42.88 - 49.87	42.65 - 42.86
Longitude (°E)	-3.90 - 9.48	0.08 - 6.94	-4.24 - 6.96	-0.33 - 1.92
Maximal depth (m)	0.8 - 309.7	10.3 - 180	1.2 - 124	49 - 112
Surface area (km ²)	0.08 - 577.12	0.11 - 6.52	0.29 - 57.57	0.45 - 1.21
Volume (m ³)	$5 \times 10^4 - 8.9 \times 10^{10}$	$51.4 \times 10^4 - 33.32 \times 10^7$	$12.9 \times 10^4 - 49.88 \times 10^7$	$72.7 \times 10^5 - 68.6 \times 10^6$

284

285 3.4.3.5. Calibration, uncertainty and sensitivity analysis

286 ~~The initial assessment of the quality of OKPLM simulations described in the previous section has been completed~~
 287 ~~with a sensitivity and uncertainty analysis. For e~~Calibration_ ~~and~~ uncertainty ~~and sensitivity~~ analyses were carried
 288 ~~out using~~ the package “CUSPY” (Calibration, Uncertainty analysis and Sensitivity analysis in PYthon), which
 289 is part of the software ~~suite~~environment “ALAMODE”- (Danis, 2020) and acts as an interface to the package
 290 “pyemu” (White et al., 2016, 2020).

291 Parameter values were calibrated for lakes with enough available in situ data (temperature profiles and
 292 bathymetry). Parameter values were calibrated using the Gauss-Levenberg-Marquardt algorithm and Tikhonov
 293 regularization (White et al., 2020), and the squared sum of residuals as objective function. In addition to the
 294 calibrated parameter values, the calibration process also provided posterior parameter uncertainty and composite
 295 scaled sensitivities. Composite scaled sensitivities (CSS) indicate the quantity of information provided by each
 296 parameter and the sensitivity of the model to them (Ely, 2006). The parameters with higher CSS values will have
 297 a greater impact on the resulting simulation compared to those with low CSS values. To determine the CSS values
 298 for each parameter, the Dimensionless Scaled Sensitivities (DSS) are used. DSS indicate how important an
 299 observation or how sensitive a simulated equivalent of an observation is in relation to the estimation of a parameter.
 300 Further information on these statistical measures is available in Hill (1998) and Poeter & Hill (1997). The
 301 dimensionless scaled sensitivity for i and j , i being one of the observations and j being one of the parameters, is
 302 calculated as:

$$303 \quad \text{DSS}_{i,j} = \left[\frac{\partial y'_i}{\partial b_j} \right] b_j w_i^{1/2} \quad (13)$$

where y'_i is the simulated value associated with the i th observation, b_j is the j th estimated parameter, $\frac{\partial y'_i}{\partial b_j}$ is the sensitivity of the simulated value associated with the i th observation and w_i is the weight of the i th observation.

The CSS for parameter j is calculated from DSS as follows:

$$CSS_j = \left[\frac{\sum_{i=1}^{ND} (DSS_{ij})^2 |b|}{ND} \right]^{1/2} \quad (14)$$

where ND is the number of observations and b is a vector of parameters values.

The uncertainty of the simulations (calibrated and default) was analyzed using Monte Carlo simulations. For each lake, 100 Monte Carlo simulations were carried by randomly selecting the value of the model parameters. Two parameters, *at_factor* and *sw_factor*, multiplying the meteorological input, were added to account for possible uncertainties in input data. For default simulations, the a priori distribution of the parameters was assumed to follow a normal distribution with the average value and lower and upper bounds shown in Table 2. The ranges for parameters A , B and C were estimated as four times the standard deviation of the residuals of the formulas used to estimate them according to Prats & Danis (2019). The parameters D , E and β , are expected to lie in the range 0-1 for mathematical and physical reasons. However, their respective values are highly interdependent and are difficult to identify. Given their higher uncertainty, the full 0-1 range was explored. For MAAT, *at_factor* and *sw_factor*, reasonable ranges ($\pm 10\%$) were chosen to account for meteorological data uncertainty (measurement error, errors in regionalization, etc.). For calibrated simulations, the distribution of the parameters was obtained from the calibration results.

In this study, the non-parametric Kendall's tau coefficient (significance level at 5%) was used to identify statistical associations between uncertainty values and CSS in respect to lake geomorphological characteristics (maximal depth, volume, surface area, latitude and altitude).

Table 2: Characteristics of the a priori distributions of the model parameters. Parameters with a circumflex accent indicate parameter values estimated for a particular lake according to the regionalization formulas by Prats & Danis (2019).

Parameter	Average value	Lower bound	Upper bound
A	\hat{A}	$\hat{A} - 2 \cdot 0.74$	$\hat{A} + 2 \cdot 0.74$
B	\hat{B}	$\hat{B} - 2 \cdot 0.08$	$\hat{B} + 2 \cdot 0.08$
C	\hat{C}	$\hat{C} - 2 \cdot 0.004$	$\hat{C} + 2 \cdot 0.004$
D	\hat{D}	0	1
E	\hat{E}	0	1
α	$\hat{\alpha}$	0	$\hat{\alpha} + 2 \cdot 0.08$
β	$\hat{\beta}$	0	1

<i>MAAT</i>	<i>M\hat{A}AT</i>	<i>M\hat{A}AT</i> - 2 · 0.5	<i>M\hat{A}AT</i> + 2 · 0.5
<i>at_factor</i>	1	0.9	1.1
<i>sw_factor</i>	1	0.9	1.1

324

325 4. Model performance

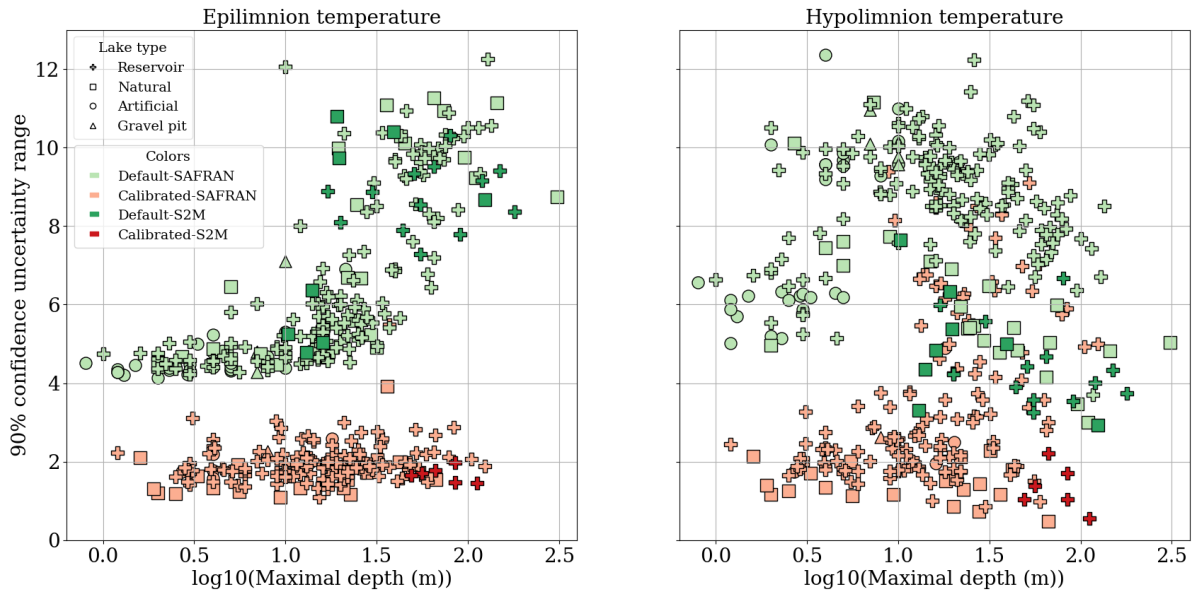
326 The performance of the OKPLM was assessed in Prats & Danis (2019) by comparing its performance to two other
327 often-applied models in lake studies, air2water and FLake. The air2water model is a semi-empirical model used
328 to calculate the epilimnion temperature of temperate lakes (Toffolon et al., 2014; Piccolroaz et al., 2013). [FLake](#)
329 [FLake](#) is a one-dimensional (1D) hydrodynamic lake model for simulating temperature vertical profiles and mixing
330 conditions in lakes (Mironov, 2008). To assess their performances, ~~the three~~ both models were run ~~with default~~
331 ~~parameter values~~ between 1999 and 2016 over ~~two~~ sets of ~~409~~ French lakes of different types (reservoirs, natural
332 lakes, ~~ponds, quarry lakes~~ ~~artificial lakes~~ and gravel pits): [a group of with temperature measurements including](#)
333 [five lakes with continuous profile measurements, and a group of 404 lakes with less frequent temperature](#)
334 [measurements. The performance assessment was limited to the period of 1999-2016 due to the availability of water](#)
335 [temperature data \(in situ and satellite\) during that specific timeframe. The scarcity of in situ water temperature](#)
336 [measurements before 1999 applies to the entire set of lakes. However, it is important to note that long-term in situ](#)
337 [water temperature data is available for a few large lakes, which was used to assess the performance of the three](#)
338 [models](#) (Prats & Danis, 2015). [The OKPLM was run with the “default” parameter values given by the](#)
339 [parameterization in Prats & Danis \(2019\). The air2water parameter values were obtained as a function of lake](#)
340 [depth by adopting from the parametrization presented in](#) Toffolon et al. (2014). [When evaluating the model](#)
341 [performance with the set of five lakes with continuous data, air2water was also run using parameter values](#)
342 [calibrated for the individual lakes available data. FLake does not have calibration parameters. Meteorological-](#)
343 [forcing \(SAFRAN\) consisted of air temperature for the air2water model; solar radiation, vapor pressure, cloud](#)
344 [cover and wind speed for FLake; and air temperature and solar radiation for the OKPLM.](#)

345 The OKPLM, air2water and FLake simulations were assessed through comparison to in situ measurements. For
346 epilimnion temperatures, the average discrepancies calculated between OKPLM simulations and observations
347 remained below 2 °C in most cases, in contrast to the air2water and FLake models. The performance comparison
348 between the OKPLM, air2water and FLake yielded respectively median RMSE's (Root Mean Square Error) of
349 1.7, 2.3 and 2.6 °C calculated between simulations and observations of epilimnion water temperature. [Although](#)
350 [when using calibrated parameter values for air2water, median RMSE was below 1 °C in most cases.](#) For
351 hypolimnion temperatures, the median RMSEs by lake type obtained with OKPLM simulations remained below
352 2 °C, except for gravel pits (RMSE = 2.7 °C) and reservoirs (RMSE = 2.3 °C), whereas FLake yielded a median
353 RMSE of 3.3 °C. For the epilimnion, the differences between the RMSE of lake types were not significant. In
354 terms of depth, discrepancies between epilimnion temperature simulations with the OKPLM and measurements
355 were highest for lakes with a depth > 10 m and for ponds around 1 m deep. The OKPLM simulations were also
356 evaluated seasonally, in particular during summer and winter. The model simulated temperatures well with a
357 median RMSE of 1.4 and 1.6 °C in summer and winter respectively.

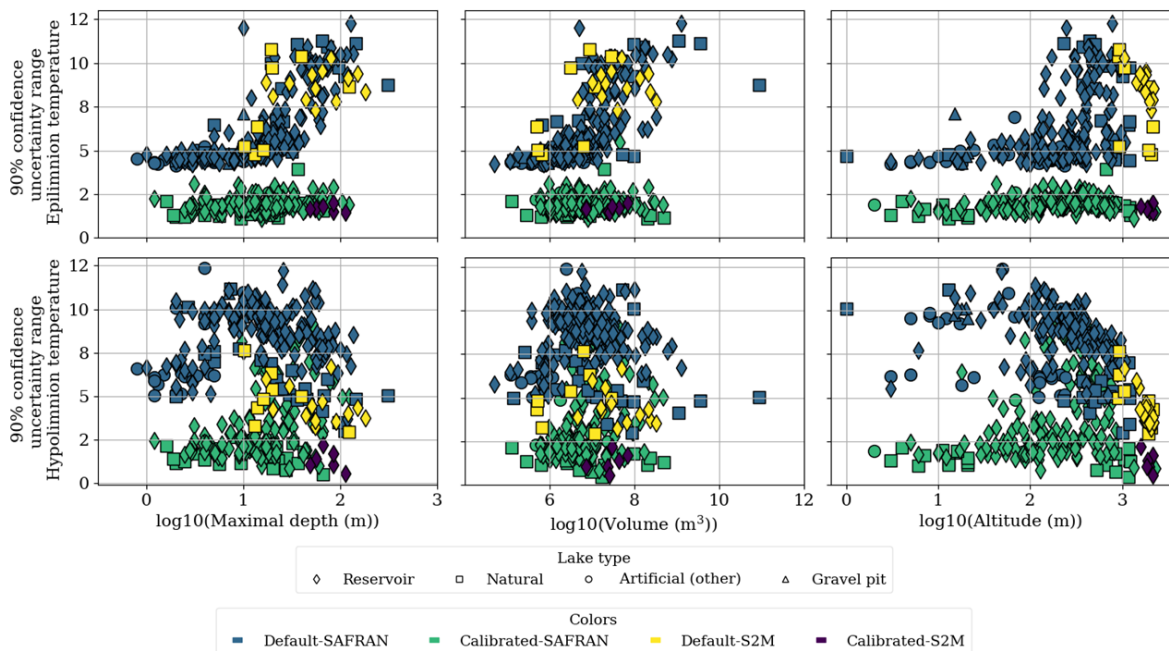
5. Uncertainty analysis

~~The uncertainty analysis revealed that,~~ Overall, for both simulations with default and calibrated model parameters, uncertainty was higher ~~and recurrent~~ for hypolimnion temperature compared to epilimnion temperature especially in reservoirs (Figure 3). In default simulations, ~~the uncertainty of simulated epilimnion temperatures values~~ showed a clear and strong relation with lake maximal depth (Figure 3, Table 3). ~~For epilimnion temperature.~~ On one hand, maximal depth had the highest Kendall's tau value of 0.64 (p -value < 0.0001), indicating a strong positive correlation with uncertainty followed by volume with a Kendall's tau of 0.59 (p -value < 0.0001). Uncertainty increased with maximal depth and volume in particular for lakes with depths greater than 10 m and volumes greater than 10^6 m^3 (Figure 3). Overall, lakes with higher maximal depths have higher volumes and are located at greater altitudes (Figures A1-A2 in Appendix A). On the other hand, moderate significant correlations were identified with surface area, altitude and latitude (Table 3). Lakes with larger surface areas and higher altitudes tend to have higher uncertainties whereas lakes located at higher latitudes tend to have lower uncertainties (Figure A3 in Appendix A). The latter can be linked to the fact that more shallow lakes are located at higher latitudes (Figure A1 in Appendix A). For default simulations of hypolimnion temperatures, uncertainty was maximal for lakes with depths around 10 m. Kendall's tau values revealed a moderate significant correlation between hypolimnion temperature uncertainty and altitude (-0.45 , p -value < 0.0001). The decrease in uncertainties with altitude can be related to the fact that lakes situated at very high altitudes are mostly deep. Further, in the present dataset, lakes with higher maximal depths occur as altitude increases (Figure A1-A2 in Appendix A).

After calibration, there was an important reduction in simulation uncertainty. For default simulations of epilimnion temperature the median of the 90% confidence uncertainty range was $5.42 \text{ }^\circ\text{C}$, while after calibration it was $1.85 \text{ }^\circ\text{C}$. For hypolimnion temperature, the median of the 90% confidence uncertainty range of default simulations was $8.5 \text{ }^\circ\text{C}$, while it was $2.32 \text{ }^\circ\text{C}$ after calibration. However, many reservoirs with depths greater than 8 m still had a much greater uncertainty (uncertainty range $> 4 \text{ }^\circ\text{C}$) than the rest of lakes after calibration. Additionally, reservoirs (and a few natural lakes) above 100 m in altitude showed the highest uncertainties in the simulation of epilimnion temperature.



385



386

Figure 3: Average 90% confidence uncertainty range for epilimnion (top panel) and hypolimnion (bottom panel) temperatures in calibrated ($n = 170$) and default ($n = 231$) simulations for the period 1959-2020.

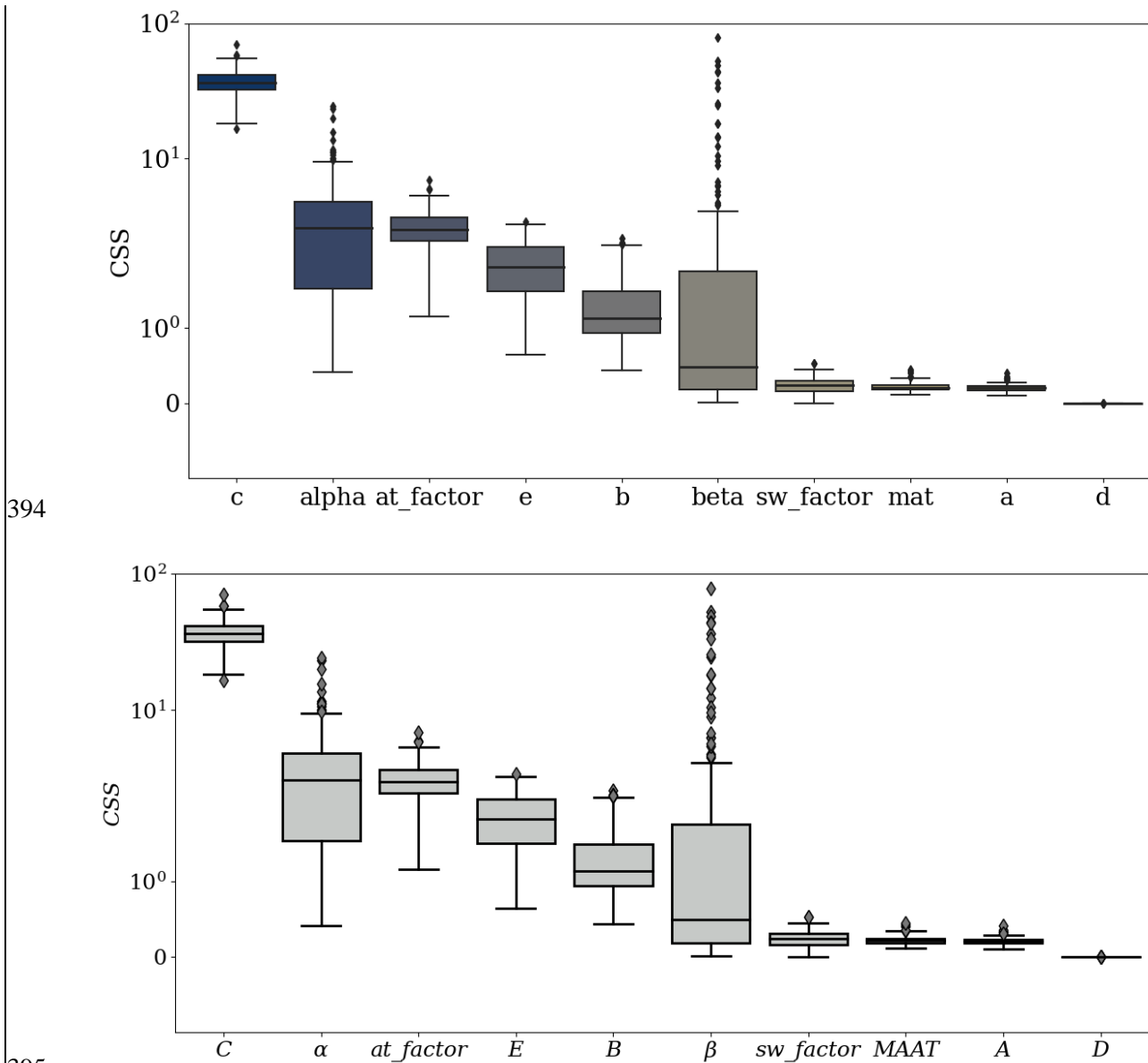
Table 3: Kendall's tau coefficients and p -values of average 90% confidence uncertainty range for epilimnion and hypolimnion temperatures obtained from default simulations (1959-2020) in respect to lakes geomorphological characteristics. For each lake, "Epilimnion uncertainty" and "Hypolimnion uncertainty" are defined as the average 90% confidence uncertainty range calculated as the difference between the 95th and 5th percentiles of the daily simulated epilimnion and hypolimnion water temperatures. The significance levels are represented as follows: *, $1.00e-02 < p\text{-value} \leq 5.00e-02$, **, $1.00e-03 < p\text{-value} \leq 1.00e-02$, *, $1.00e-04 < p\text{-value} \leq 1.00e-03$, ****: $p\text{-value} \leq 1.00e-04$. Otherwise, correlations are not significant ($p\text{-value} > 0.05$).**

	<u>Maximal depth</u> (m)	<u>Surface area</u> (km ²)	<u>Altitude</u> (m)	<u>Latitude</u> (°N)	<u>Volume</u> (m ³)
--	-----------------------------	---	------------------------	-------------------------	------------------------------------

<u>Epilimnion uncertainty</u>	<u>0.64****</u>	<u>0.31****</u>	<u>0.39****</u>	<u>-0.40****</u>	<u>0.59****</u>
<u>Hypolimnion uncertainty</u>	<u>-0.13**</u>	<u>0.05</u>	<u>-0.45****</u>	<u>0.03</u>	<u>-0.03</u>

387 **6. Sensitivity analysis**

388 The parameter to which the model was most sensitive was the parameter C (Figure 4), which multiplies solar
 389 radiation in Eq. (1). The CSS for C were an order of magnitude greater than for the next parameters with highest
 390 CSS, the parameter α and *at_factor*, both influencing the effect of air temperature on simulated water temperature.
 391 Other parameters to which the model was somewhat sensitive were *E*, *B* and β . The model was quite insensitive
 392 to *sw_factor*, *MAAT* and *A*. The parameter *D*, with CSS several orders of magnitude smaller than the other
 393 parameters, was unidentifiable.



394
395
Figure 4: Composite scaled sensitivities (CSS) for each parameter. The boxplots indicate the distribution of CSS between the simulations calibrated for different lakes. The y-axis is in logarithmic form.

396 The model tended to be more sensitive to the parameter values in the case of reservoirs than in the case of natural
397 lakes—(Figure 5, Figures A4-A7 in Appendix A). Some parameters showed a dependency on lakes
398 geomorphological characteristics. With the exception of a weak correlation with altitude (Kendall's tau = 0.18),
399 there was no significant dependence between the parameter C and lakes geomorphological characteristics (Table
400 4, Figure A4 in Appendix A). The parameter α being parametrized as a function of lake volume, surface area and
401 altitude reflects the thermal inertia of the lake. It showed a clear highly significant dependency primarily on lake
402 depth (Kendall's tau = 0.47) followed by altitude (Kendall's tau = 0.4) and volume (Kendall's tau = 0.39)—(Figure
403 5, Table 4). The increase of model sensitivity to the parameter α primarily with depth as well as altitude and volume
404 propagated to the default simulations and explain the increased uncertainty can be related with the increase in
405 uncertainty with these same geomorphological characteristics depth in the default simulations. The parameter
406 at factor, was weakly but significantly correlated with all lakes geomorphological characteristics except for
407 latitude with which no correlation was found (Figure 5, Table 4, Figures A4-A7 in Appendix A). Some parameters
408 (α , β) also showed a dependency on lake depth. The increase of model sensitivity to the parameter α with depth
409 can be related with the increase in uncertainty with depth in the default simulations. In the case of the parameter
410 β , CSS were mostly low for the parameter β , with a median value of 0.49. However, except for a few for some
411 reservoirs and artificial lakes that scored very high water bodies CSS could attain very high values. The sensitivity
412 of β displayed a weak but significant correlation with lakes geomorphological characteristics, except for volume
413 (Table 4).

414 Although the model in general was not very sensitive to the values of the parameters most directly related with
415 hypolimnion temperatures (D , E , β), the quality of hypolimnion temperature was greatly improved through
416 calibration. This would seem to indicate that the quality of simulated hypolimnion temperature was improved
417 through the improvement of epilimnion temperature simulations.

Table 4: Kendall's tau coefficients and p -values of CSS for model parameters values and drivers obtained from calibrated simulations (1959-2020) in respect to lakes geomorphological characteristics. The significance levels are represented as follows: *: $1.00e-02 < p\text{-value} \leq 5.00e-02$, **: $1.00e-03 < p\text{-value} \leq 1.00e-02$, *: $1.00e-04 < p\text{-value} \leq 1.00e-03$, ****: $p\text{-value} < 1.00e-04$. Otherwise, correlations are not significant ($p\text{-value} > 0.05$).**

	<u>Maximal depth</u> <u>(m)</u>	<u>Surface area</u> <u>(km²)</u>	<u>Altitude</u> <u>(m)</u>	<u>Latitude</u> <u>(°N)</u>	<u>Volume</u> <u>(m³)</u>
<u>CSS_A</u>	<u>0.02</u>	<u>-0.1</u>	<u>0.14**</u>	<u>-0.08</u>	<u>-0.07</u>
<u>CSS_B</u>	<u>0.09</u>	<u>-0.04</u>	<u>0.14**</u>	<u>-0.14**</u>	<u>0.02</u>
<u>CSS_C</u>	<u>-0.04</u>	<u>-0.09</u>	<u>0.18***</u>	<u>-0.05</u>	<u>-0.1</u>
<u>CSS_D</u>	<u>-0.12*</u>	<u>0.02</u>	<u>-0.14**</u>	<u>0.06</u>	<u>-0.1</u>
<u>CSS_E</u>	<u>-0.01</u>	<u>-0.001</u>	<u>0.02</u>	<u>0.0003</u>	<u>-0.03</u>
<u>CSS_{α}</u>	<u>0.47****</u>	<u>0.07</u>	<u>0.4****</u>	<u>-0.23****</u>	<u>0.39****</u>
<u>CSS_{β}</u>	<u>0.16**</u>	<u>-0.12*</u>	<u>0.22****</u>	<u>-0.19***</u>	<u>0.05</u>
<u>CSS_{at factor}</u>	<u>-0.25****</u>	<u>-0.14**</u>	<u>-0.13*</u>	<u>0.04</u>	<u>-0.28****</u>
<u>CSS_{sw factor}</u>	<u>-0.22****</u>	<u>-0.06</u>	<u>-0.14**</u>	<u>0.06</u>	<u>-0.2****</u>
<u>CSS_{MAAT}</u>	<u>-0.09</u>	<u>-0.13**</u>	<u>0.13*</u>	<u>-0.02</u>	<u>-0.15**</u>

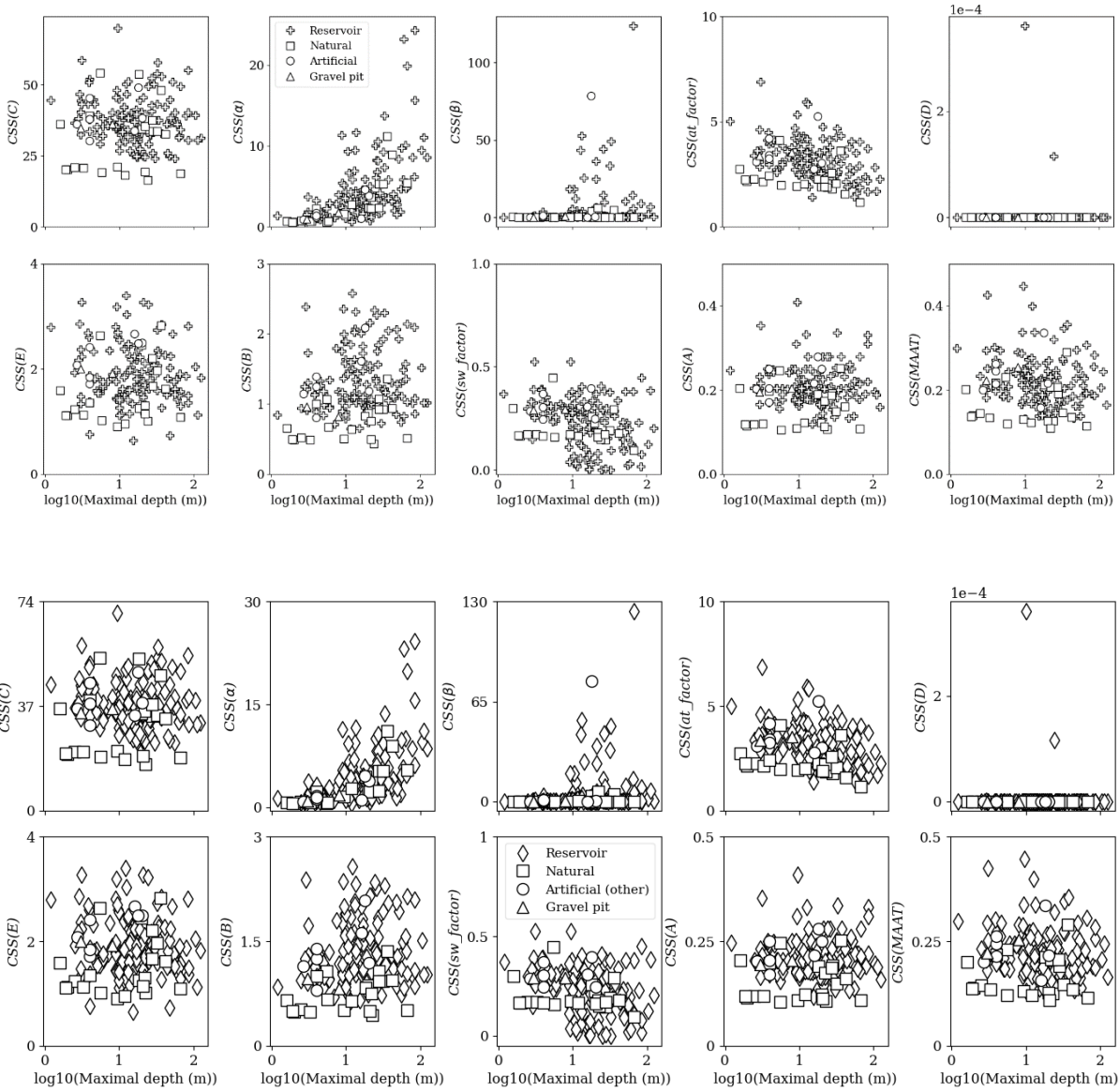


Figure 5 : Composite scaled sensitivities (CSS) for each model parameter as a function of maximal depth.

421 **7. Discussion and implications**

422 Lakes are undeniably changing under climate change and long-term future projections show that the shifts in
 423 ecosystem functioning will continue with aggravated alterations (Woolway & Merchant, 2019). In particular, given
 424 the key role of ~~warming~~ lake water temperature in regulating ecosystem processes, its warming has become a
 425 response that is crucial to monitor, explore and understand. Hence, the importance of developing or adopting
 426 approaches, such as numerical models, that will provide long-term information about water temperature and allow
 427 us to understand the thermal response of lakes to climate change.

428 Here we used a semi-empirical model, the OKPLM, to simulate six decades of epilimnion and hypolimnion water
 429 temperatures in French lakes. In comparison to similar models, overall, the OKPLM provides acceptable
 430 estimations of water temperatures, with better results for epilimnion temperatures. The values of the RMSEs

431 provided in Prats & Danis (2019) and obtained between OKPLM simulations and observations are comparable to
432 values found in studies applying complex hydrodynamic lake models (Read et al., 2014; Fang et al., 2012). ~~The~~
433 ~~analysis revealed that~~When using the default parameter values, the uncertainty associated ~~with both~~ with
434 epilimnion ~~and hypolimnion~~ temperature simulations was ~~significantly~~highly related to all geomorphological
435 characteristics however, it was especially strongly correlated to lake maximal ~~lake~~ depth. In contrast,~~While the~~
436 uncertainty in the hypolimnion simulations had a significant correlation solely with altitude and maximal depth.
437 The importance of this correlation was especially noteworthy in the case of reservoirs located in low-altitude
438 regions where uncertainties were the lowest. While the association between hypolimnion uncertainty and maximal
439 depth exhibited only a weak correlation, the instances of highest uncertainties were predominantly found in
440 reservoirs having maximal depths around 10 m. The uncertainty in hypolimnion simulations is more important and
441 especially associated with reservoirs having maximal depths > 8 m. The correlations found between lakes
442 geomorphological characteristics and simulations uncertainties suggests that there might be systematic biases in
443 the definition of model parameters or in the forcing data. The calibration of model parameters significantly reduced
444 the uncertainties yet, for hypolimnion temperatures, they remained considerably high and increased with depth
445 especially in reservoirs.

446 The high levels of uncertainty found in reservoirs could be somewhat attributed to the lack of consideration of
447 water level fluctuations in the model. In contrast to other ~~lakes~~waterbodies (e.g., natural lakes, artificial lakes and
448 gravel pits) reservoirs experience significant variations in their water level, which influences the heat budget and
449 hence their thermal regime. Therefore, even under similar meteorological conditions lakes and reservoirs could
450 have different thermal behaviors (Nowlin et al., 2004). In reservoirs, the discharge depth is a driver of thermal
451 structure. Deep discharges could contribute to warmer bottom waters (Carr et al., 2020) whereas in some cases if
452 the reservoir is shallow or if the discharge depth is not deep, it could demonstrate lake-like thermal behavior. This
453 does not necessarily mean that, in this case, the entire functioning of the reservoir resembles one of a natural lake;
454 there are still differences to consider (Detmer et al., 2022).

455 The application of the OKPLM should be made with caution given its performance and depending on the objective
456 of the study. The model does not take into account a complete set of meteorological forcing (e.g., with cloud cover,
457 relative humidity and wind speed and direction) or other variables (e.g., inflow and outflow rates or water level
458 fluctuations, inflow discharge depth and inflow temperature) that could influence the thermal structure of the
459 ecosystem (Yang et al., 2020; Carr et al., 2020). Furthermore, the OKPLM was parametrized for a specific set of
460 lakes with particular geomorphological characteristics. Thus, it would be advisable to apply the model over lakes
461 with similar characteristics. If the aim is to conduct a long-term regional or global study for studying general
462 patterns of climate change impacts over a large number of study sites, the utilization of semi-empirical models
463 such as the OKPLM is the most suitable choice. Although complex, deterministic or process-based models provide
464 a more accurate representation of thermal conditions, applying these models over several study sites and for long
465 periods is usually hindered by the scarcity of the required input data. The increased complexity of these models
466 (with reference to an increased number of model parameters) is beneficial for representing additional ecosystem
467 processes. Yet the greater number of model parameters, increases the sensitivity of models and demands more
468 calibration efforts (Lindenschmidt, 2006). Furthermore, a reduction in model errors is sometimes associated with
469 an increased complexity in model structure; however, this is not always consistent since a complex model does
470 not necessarily provide better estimations and thus lower errors than a simple model (Snowling and Kramer, 2001).

471 Our goal in publishing the present dataset is to expand knowledge about the water temperature of French lakes and
472 provide data, with enough details and reliability, that it could be implemented in different studies where water
473 temperature is implicated for understanding specific processes or interactions, in particular under climate change.
474 Hence the significance of the present findings. The present study, making use of a semi-empirical model to provide
475 long-term data about water temperature, was necessary for several reasons. Equipping a large number of lakes
476 with thermal sensors is challenging and labor-intensive, it comes with a high financial cost that is often not
477 available. Consequently, historical and even current water temperature datasets are often scarce, which can be
478 problematic for studying the impact of climate change, as it requires high frequency data over a long duration of
479 time for accurate analysis. In general, the higher the sampling frequency and duration, the better the data is suited
480 to estimate or analyze specific processes or warming trends. The sampling frequency and length of a dataset have
481 been shown to play a role in determining the accuracy of estimating warming trends where time series longer than
482 30 years seem to be the most appropriate (Gray et al., 2018). Although, the duration and frequency of a dataset
483 have a major role in reflecting accurate representations, their influence is scarcely addressed when it comes to
484 climate change studies related to warming trends in water temperature.

485 This dataset is very useful for climate change studies; it could be used for developing and analyzing several
486 temperature indicators (e.g., annual or seasonal maximal and minimal temperature values, temperature exceeding
487 certain thresholds with biological implications, etc.). Further, mixing and stratification dynamics are important to
488 characterize as they drive lake biogeochemistry. Among other processes, they influence the distribution of
489 nutrients, primary productivity and the composition of phytoplankton and zooplankton communities along the
490 water column (Judd et al., 2005). With the LakeTSim dataset, it is possible to classify the mixing regime of lakes
491 and investigate possible triggers of regime shifts.

492 **8. Data usage**

493 The LakeTSim dataset comprises water temperature simulations for natural lakes ($n = 54$), reservoirs ($n = 302$),
494 gravel pits ($n = 7$), and other artificial lakes (e.g., ponds and quarry lakes, $n = 38$). The simulations are for both the
495 epi- and hypolimnion. Lakes that are fully mixed throughout the year (typically, shallower lakes) have the same
496 temperature value for both layers. More generally, the delta of temperature can be used to calculate mixing regimes
497 (Sharaf et al., in prep.).

498 The lakes in the dataset were selected because they are monitored as part of the European Water Framework
499 Directive (Directive 2000/60/EC). The majority of the 401 lakes are non-natural and some were only created after
500 1959 (i.e., the start of our simulations). We compiled the initial filling years for 282 of these 347 non-natural lakes
501 (269 reservoirs and 13 artificial lakes, Figure A8 in Appendix A) in Table S1 (see Supplement) to be used as a
502 companion dataset to LakeTSim. The filling years were sourced from <https://www.barrages-cfbr.eu> for 179 of the
503 lakes and from the PLAN_DEAU database for 103 of the lakes; the information was not available for 33 reservoirs,
504 7 gravel pits and 25 other artificial lakes of the LakeTSim dataset.

505 The median filling date was 1962 and 67% of the lakes with known filling dates were filled by 1980. While the
506 complete simulations ranging from 1959 to 2020 can also be used as theoretical lake temperature for comparison
507 across similar periods, we recommend that users of LakeTSim data for reservoir and artificial lake simulations
508 consider the initial filling dates provided in Table S1 to filter out years from the simulations during which lakes
509 were not filled yet.

510 Additionally, users should be aware that some reservoirs might be drained completely at certain intervals (e.g.,
511 every 10 years) for maintenance and inspection purposes. Finally, as mentioned in the discussion, some of the
512 lakes in the dataset experience artificial (e.g., in reservoirs) or natural (e.g., in some smaller ponds) water level
513 fluctuations, and potential intermittent dry-periods lasting weeks or months; none of these hydrological processes
514 are accounted for in the simulations.

515 9. Code availability

516 The respective codes for the “CUSPY” (Prats-Rodríguez and Danis, 2023a) and “OKPLM” (Prats-Rodríguez and
517 Danis, 2023b) packages, which can be used to conduct sensitivity and uncertainty analysis and to run the OKP
518 Lake Model, are available at <https://github.com/inrae/ALAMODE-cuspy> and
519 <https://github.com/inrae/ALAMODE-okp> as well as ZENODO.

520 10. Data availability

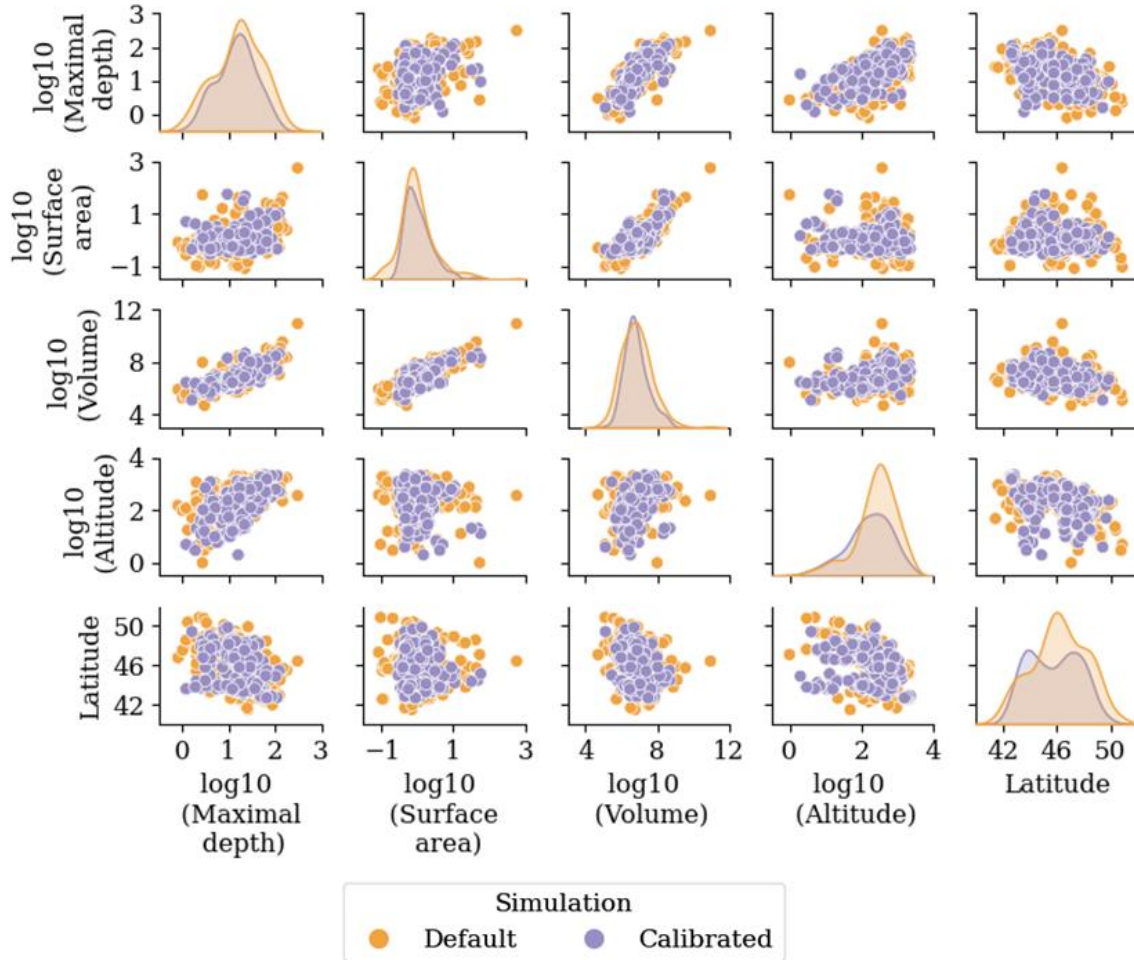
521 The LakeTSim dataset (Sharaf et al., 2023) for epilimnion and hypolimnion water temperature simulations and
522 supporting information are available at [doi:10.57745/OF9WXR](https://doi.org/10.57745/OF9WXR). The file “00_Data_description.txt” contains a
523 description of the dataset. The geographical (longitude and latitude) and morphological (surface area, volume and
524 maximum depth) data for the 401 lakes are presented in the file “01_Lake_data.txt” in addition to the name, type,
525 altitude and the identification code for each lake. The data are located in two main folders: “02_Temperature_data”
526 containing daily epilimnion (tepi) and hypolimnion (thyp) temperatures simulated with the OKPLM and
527 “03_Uncertainty_data” containing daily tepi and thyp uncertainties. In each folder, ~~the data for daily epilimnion~~
528 ~~(tepi) and hypolimnion (thyp) temperatures simulations and their uncertainties~~ ~~with the OKPLM~~ are presented
529 in text files available in the folders “002_LakeTSim_SAFRAN_OKPdefault_data”,
530 “013_LakeTSim_SAFRAN_OKPcalibrated_data”, “024_LakeTSim_S2M_OKPdefault_data” and
531 “035_LakeTSim_S2M_OKPcalibrated_data”. The name of each file within these folders includes is named
532 according to the identification code of the lake. From 2024, the data will be visible from a dashboard. The link to
533 the dashboard will be accessible from data.ecla.inrae.fr.

534 11. Conclusions

535 We present the LakeTSim dataset and the semi-empirical OKP Lake Model for simulating water temperature in
536 Lakes. We applied the model over a set of 401 French lakes for the period 1959-2020 to derive daily simulations
537 of epilimnion and hypolimnion water temperatures, here referred to as the LakeTSim dataset. Previous efforts to
538 assess the model’s performance show an overall acceptable representation of epilimnion and hypolimnion
539 temperatures when compared to in situ measurements. The uncertainty analysis of simulations demonstrates that
540 more higher uncertainties are found for is associated, by order of relative importance: firstly with (1) default
541 simulations, secondly (2) hypolimnion compared to epilimnion temperatures and, thirdly (3) deep lakes, in
542 particular reservoirs (maximal depth greater than > 108 m for epilimnion temperature and around 10 m for
543 hypolimnion temperature simulated with default model parameters). Although the calibration significantly
544 decreases the uncertainties related to both the epilimnion and hypolimnion, in some cases they are still considerable
545 for the latter in the hypolimnion. Based on these results and if enough observation data are available, optimally we
546 recommend the use of the OKPLM over for shallow (maximal depth < 8 m) lakes with calibrated model
547 parameters. However, if applied in its default or even calibrated configuration over deep lakes, one should be

548 aware of the presented limitations and address them in the analysis. The LakeTSim dataset is valuable for assessing
 549 the impact of climate change on lakes thermal functioning, which is often hindered by the lack of water temperature
 550 observations. The present dataset will provide new insights about the thermal behavior of French lakes, which can
 551 provide useful context. ~~This will be of great advantage~~ for stakeholders; as they design it should allow them to take
 552 ~~better~~ management strategies in a context of ~~under~~ climate change.

553 **12. Appendix A**



554 **Figure A1: Scatter plots of lakes ($n = 401$) geomorphological characteristics: Maximal depth (m), Surface area (km²), volume (m³), altitude (m) and latitude (°N).**

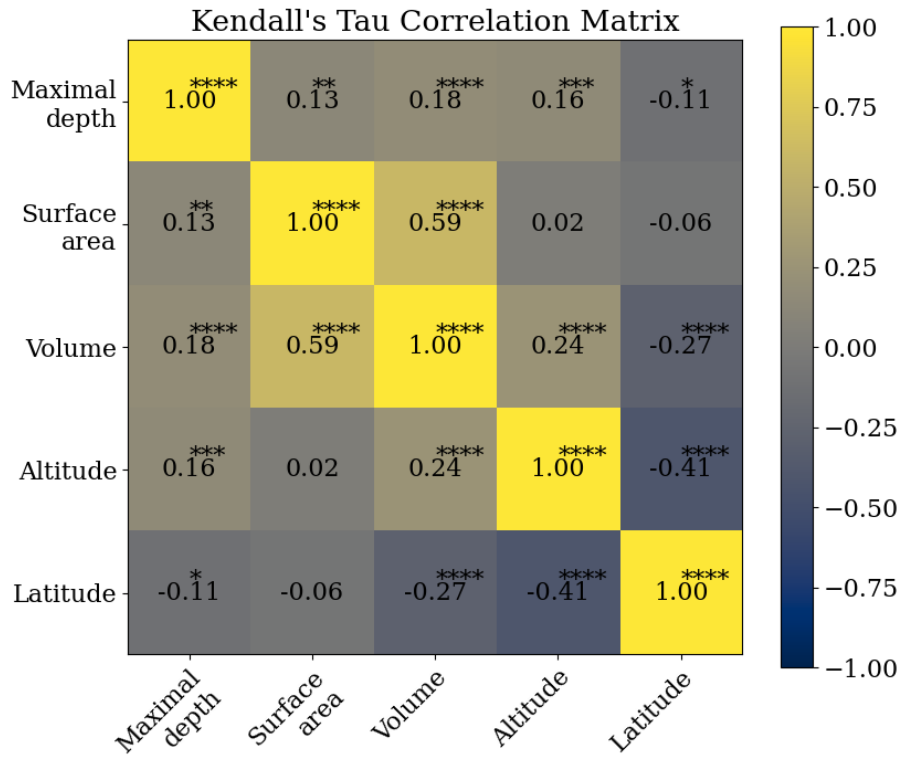


Figure A2: Kendall's tau correlation matrix of the geomorphological characteristics of lakes simulated in "default" mode ($n = 231$): Maximal depth (m), Surface area (km^2), volume (m^3), altitude (m) and latitude ($^\circ\text{N}$). The significance levels are represented as follows: *: $1.00\text{e-}02 < p\text{-value} \leq 5.00\text{e-}02$, **: $1.00\text{e-}03 < p\text{-value} \leq 1.00\text{e-}02$, *: $1.00\text{e-}04 < p\text{-value} \leq 1.00\text{e-}03$, ****: $p\text{-value} \leq 1.00\text{e-}04$. Otherwise, correlations are not significant ($p\text{-value} > 0.05$).**

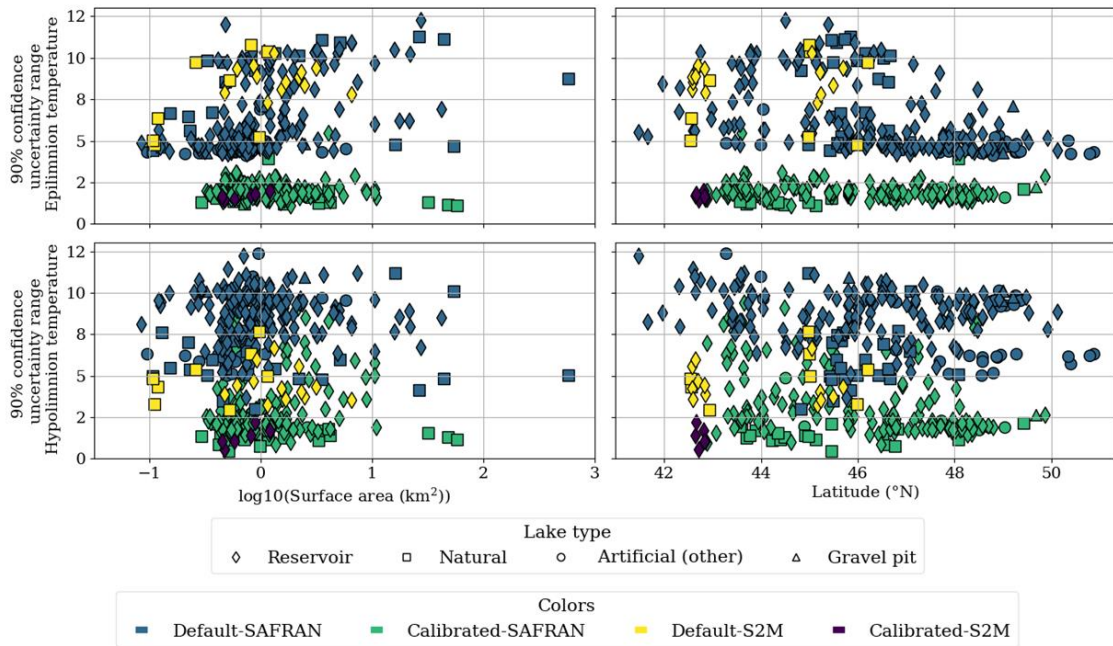


Figure A3: Average 90% confidence uncertainty range for epilimnion (top panel) and hypolimnion (bottom panel) temperatures in calibrated ($n = 170$) and default ($n = 231$) simulations for the period 1959-2020 as a function of surface area (km^2) and latitude ($^\circ\text{N}$).

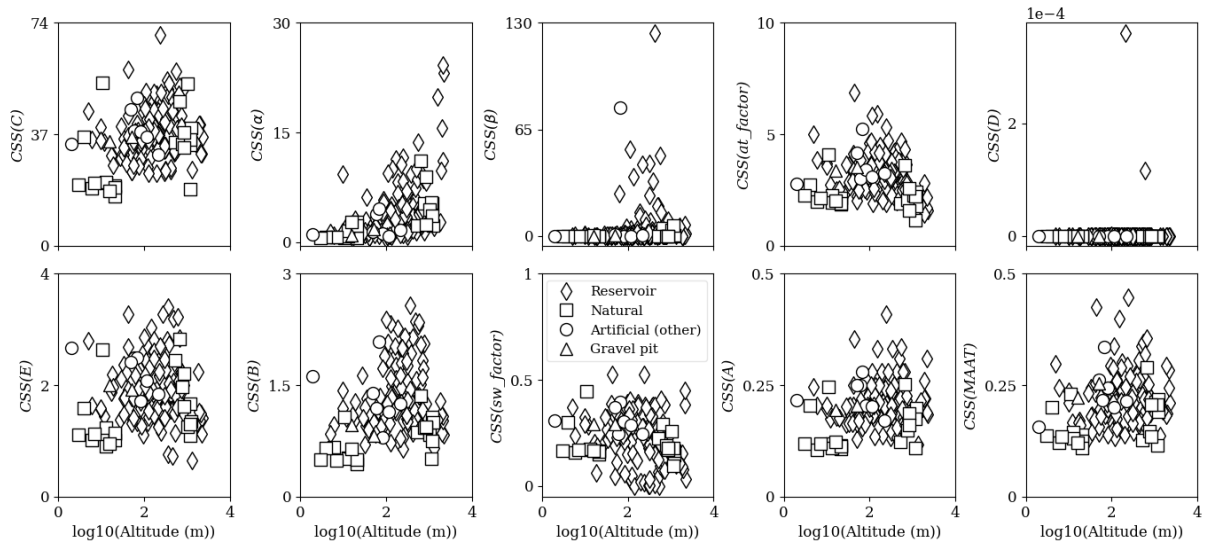


Figure A4: Composite scaled sensitivities (CSS) for each model parameter as a function of altitude.

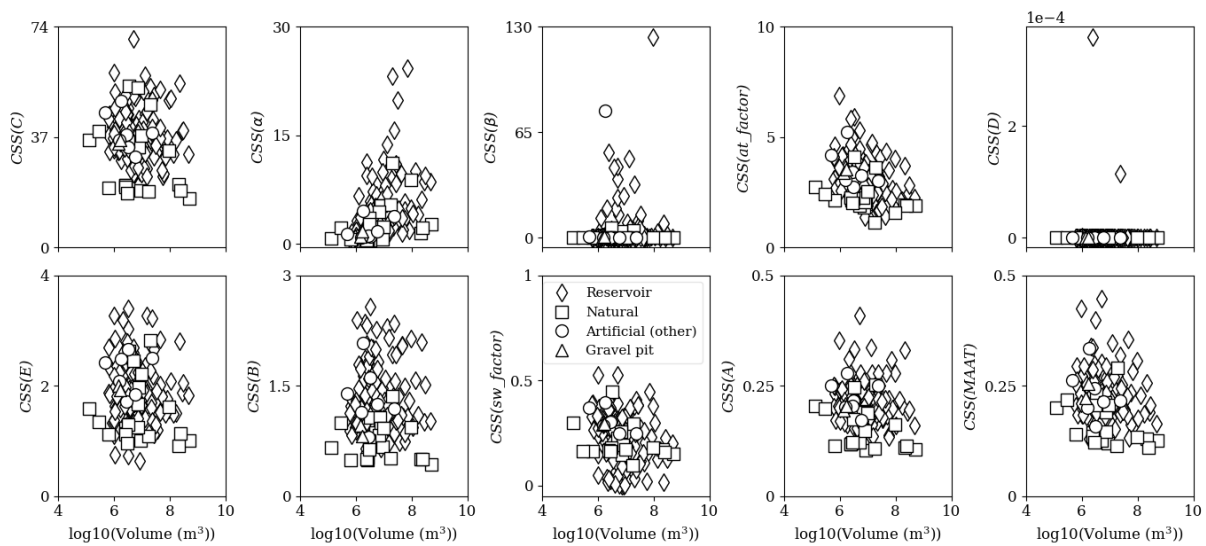


Figure A5: Composite scaled sensitivities (CSS) for each model parameter as a function of volume.

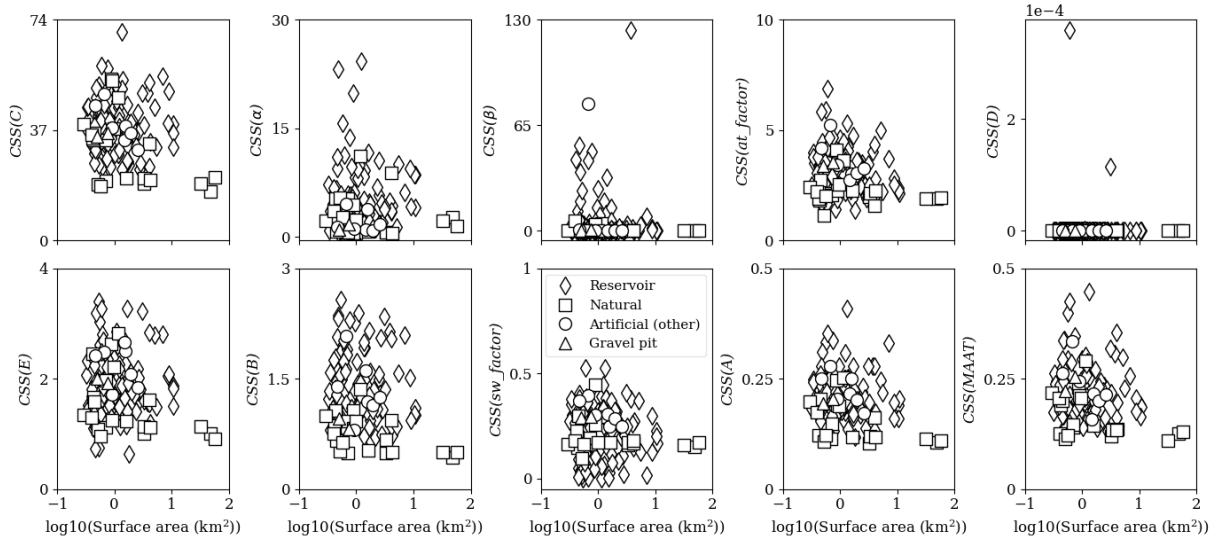


Figure A6: Composite scaled sensitivities (CSS) for each model parameter as a function of surface area.

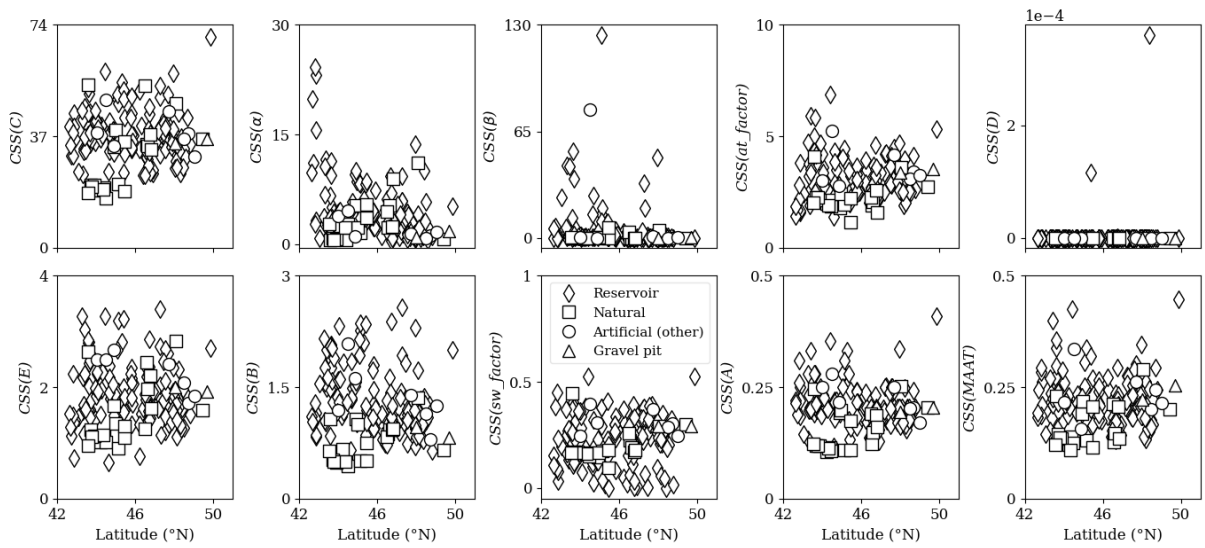
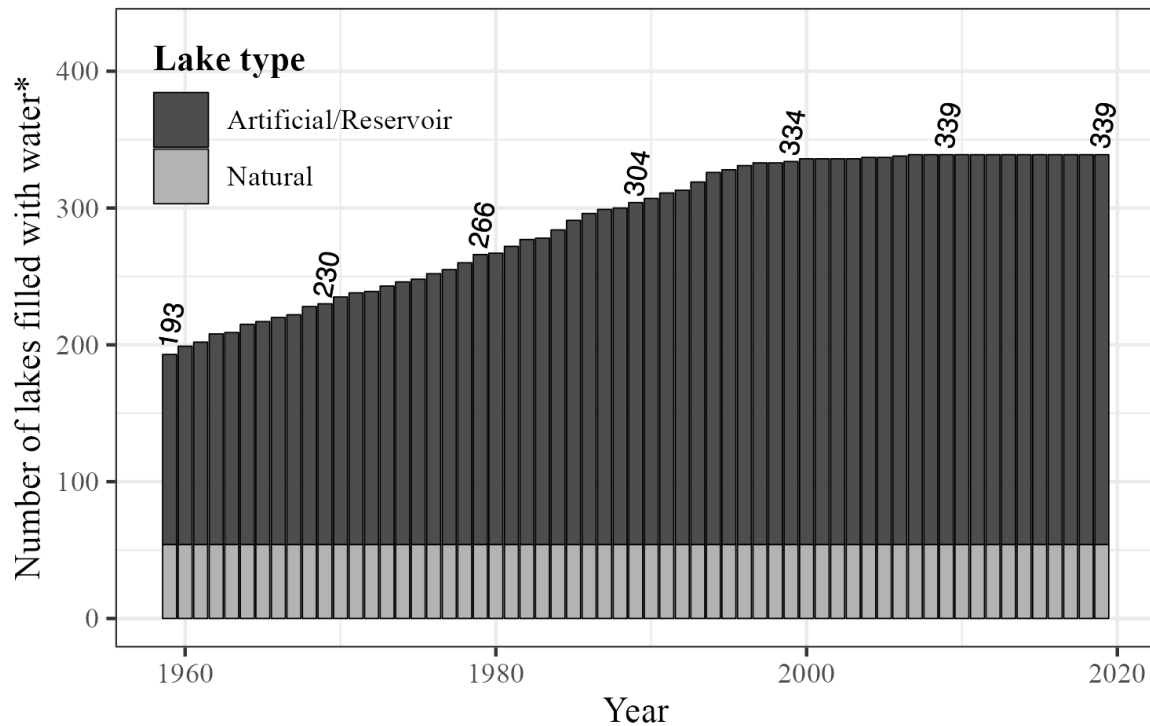


Figure A7: Composite scaled sensitivities (CSS) for each model parameter as a function of latitude.



* 7 gravel pits, 33 reservoirs & 25 other artificial lakes with no information on filling year.

Figure A8: Distribution of initial filling years for lakes (e.g., reservoirs, gravel pits and other artificial lakes) of the LakeTSim dataset.

555 13. Author contributions

556 NS wrote the original manuscript with input from JP and PAD. NS, JP and PAD discussed the results. JP developed
 557 and carried out the implementation of the OKP Lake Model and the uncertainties computation in ALAMODE. JP
 558 and NS performed the simulations and provided uncertainty analysis results with SAFRAN and S2M data
 559 respectively. JP and NS implemented respectively the integration of SAFRAN and S2M data in ALAMODE. NS
 560 prepared the LakeTSim dataset. JP and NS provided the uncertainty and sensitivity analysis. PAD designed,
 561 contributed and supervised the implementation of S2M data in ALAMODE for forcing the OKPLM when
 562 simulating high altitude lakes. -PAD supervised the findings of this work. RB proposed and contributed to the
 563 integration of the data consisting of initial filling dates of reservoirs and other artificial lakes in the manuscript.
 564 NR and TT supervised and contributed to the implementation of simulation results in the database. NR processed
 565 S2M data and compiled the data for initial filling years of reservoirs and other artificial lakes. NR and TT prepared
 566 the doi for the LakeTSim dataset. TP conducted the fieldwork for the monitoring, acquisition and verification of
 567 in situ temperature data. All authors reviewed, edited and approved the final paper.

568 14. Competing interests

569 The authors declare that they have no conflict of interest.

570 **15. Acknowledgments**

571 The authors thank Météo-France for providing SAFRAN and S2M meteorological data, Matthieu Vernay for his
572 feedback on the utilization of S2M data and the “Réseau Lacs Sentinelles” for providing bathymetry data for
573 mountain lakes.

574 **16. Financial support**

575 The authors were supported by OFB (Office Français de la Biodiversité), SEGULA Technologies, INRAE (Institut
576 National de Recherche pour l’Agriculture, l’Alimentation et l’environnement) and Pôle R&D_ECLA
577 (ECosystèmes LAcustres).

578 **17. References**

- 579 Adrian, R., O’Reilly, C. M., Zagarese, H., Baines, S. B., Hessen, D. O., Keller, W., Livingstone, D. M.,
580 Sommaruga, R., Straile, D., Van Donk, E., Weyhenmeyer, G. A., and Winder, M.: Lakes as sentinels of climate
581 change, *Limnol. Oceanogr.*, 54, 2283–2297, https://doi.org/10.4319/lo.2009.54.6_part_2.2283, 2009.
- 582 Allan, M. G., Hamilton, D. P., Trolle, D., Muraoka, K., and McBride, C.: Spatial heterogeneity in geothermally-
583 influenced lakes derived from atmospherically corrected Landsat thermal imagery and three-dimensional
584 hydrodynamic modelling, *Int. J. Appl. Earth Obs. Geoinf.*, 50, 106–116, <https://doi.org/10.1016/j.jag.2016.03.006>,
585 2016.
- 586 Babbar-Sebens, M., Li, L., Song, K., and Xie, S.: On the Use of Landsat-5 TM Satellite for Assimilating Water
587 Temperature Observations in 3D Hydrodynamic Model of Small Inland Reservoir in Midwestern US, *Adv.*
588 *Remote Sens.*, 02, 214–227, <https://doi.org/10.4236/ars.2013.23024>, 2013.
- 589 Carr, M. K., Sadeghian, A., Lindenschmidt, K. E., Rinke, K., and Morales-Marin, L.: Impacts of Varying Dam
590 Outflow Elevations on Water Temperature, Dissolved Oxygen, and Nutrient Distributions in a Large Prairie
591 Reservoir, *Environ. Eng. Sci.*, 37, 78–97, <https://doi.org/10.1089/ees.2019.0146>, 2020.
- 592 Danis, P.: Rapport d ’avancement sur les outils de modélisation thermique, 1–8 pp., <https://doi.org/hal-03253847>,
593 2020.
- 594 Daufresne, M., Lengfellner, K., and Sommer, U.: Global warming benefits the small in aquatic ecosystems, *Proc.*
595 *Natl. Acad. Sci.*, 106, 12788–12793, <https://doi.org/10.1073/pnas.0902080106>, 2009.
- 596 Detmer, T. M., Parkos, J. J., and Wahl, D. H.: Long-term data show effects of atmospheric temperature anomaly
597 and reservoir size on water temperature, thermal structure, and dissolved oxygen, *Aquat. Sci.*, 84, 1–13,
598 <https://doi.org/10.1007/s00027-021-00835-2>, 2022.
- 599 Durand, Y., Brun, E., Merindol, L., Guyomarc’h, G., Lesaffre, B., and Martin, E.: A meteorological estimation of
600 relevant parameters for snow models, *Ann. Glaciol.*, 18, 65–71, <https://doi.org/10.3189/S0260305500011277>,
601 1993.
- 602 Ely, D. M.: Analysis of Sensitivity of Simulated Recharge to Selected Parameters for Seven Watersheds Modeled
603 Using the Precipitation-Runoff Modeling System, U.S. Geological Survey Scientific Investigations Rep, 21 pp.,
604 2006.
- 605 Fang, X., Alam, S. R., Stefan, H. G., Jiang, L., Jacobson, P. C., and Pereira, D. L.: Simulations of water quality
606 and oxythermal cisco habitat in Minnesota lakes under past and future climate scenarios, *Water Qual. Res. J.*
607 *Canada*, 47, 375–388, <https://doi.org/10.2166/wqrjc.2012.031>, 2012.
- 608 Gray, D. K., Hampton, S. E., O’Reilly, C. M., Sharma, S., and Cohen, R. S.: How do data collection and processing
609 methods impact the accuracy of long-term trend estimation in lake surface-water temperatures?, *Limnol.*
610 *Oceanogr. Methods*, 16, 504–515, <https://doi.org/10.1002/lom3.10262>, 2018.
- 611 Griffith, A. W. and Gobler, C. J.: Harmful algal blooms: A climate change co-stressor in marine and freshwater
612 ecosystems, *Harmful Algae*, 91, 101590, <https://doi.org/10.1016/j.hal.2019.03.008>, 2020.
- 613 Halverson, G. H., Lee, C. M., Hestir, E. L., Hulley, G. C., Cawse-Nicholson, K., Hook, S. J., Bergamaschi, B. A.,
614 Acuña, S., Tufillaro, N. B., Radocinski, R. G., Rivera, G., and Sommer, T. R.: Decline in Thermal Habitat
615 Conditions for the Endangered Delta Smelt as Seen from Landsat Satellites (1985–2019), *Environ. Sci. Technol.*,

616 56, 185–193, <https://doi.org/10.1021/acs.est.1c02837>, 2022.

617 Havens, K. and Jeppesen, E.: Ecological responses of lakes to climate change, *Water*, 10, 917,
618 <https://doi.org/10.3390/w10070917>, 2018.

619 Hill, M. C.: Methods and guidelines for effective model calibration: U.S. Geological Survey Water-Resources
620 Investigations Report 98-4005, 90 pp., <https://doi.org/10.3133/wri984005>, 1998.

621 Hipsey, M. R., Bruce, L. C., Boon, C., Busch, B., Carey, C. C., Hamilton, D. P., Hanson, P. C., Read, J. S., De
622 Sousa, E., Weber, M., and Winslow, L. A.: A General Lake Model (GLM 3.0) for linking with high-frequency
623 sensor data from the Global Lake Ecological Observatory Network (GLEON), *Geosci. Model Dev.*, 12, 473–523,
624 <https://doi.org/10.5194/gmd-12-473-2019>, 2019.

625 Janssen, A. B. G., Hilt, S., Kosten, S., de Klein, J. J. M., Paerl, H. W., and Van de Waal, D. B.: Shifting states,
626 shifting services: Linking regime shifts to changes in ecosystem services of shallow lakes, *Freshw. Biol.*, 66, 1–
627 12, <https://doi.org/10.1111/fwb.13582>, 2021.

628 Javaheri, A., Babbar-Sebens, M., and Miller, R. N.: From skin to bulk: An adjustment technique for assimilation
629 of satellite-derived temperature observations in numerical models of small inland water bodies, *Adv. Water
630 Resour.*, 92, 284–298, <https://doi.org/10.1016/j.advwatres.2016.03.012>, 2016.

631 Judd, K. E., Adams, H. E., Bosch, N. S., Kostrzewski, J. M., Scott, C. E., Schultz, B. M., Wang, D. H., and Kling,
632 G. W.: A case history: Effects of mixing regime on nutrient dynamics and community structure in third sister lake,
633 michigan during late winter and early spring 2003, *Lake Reserv. Manag.*, 21, 316–329,
634 <https://doi.org/10.1080/07438140509354437>, 2005.

635 Kettle, H., Thompson, R., Anderson, N. J., and Livingstone, D. M.: Empirical modeling of summer lake surface
636 temperatures in southwest Greenland, *Limnol. Oceanogr.*, 49, 271–282,
637 <https://doi.org/10.4319/lo.2004.49.1.0271>, 2004.

638 Kharouba, H. M., Ehrlén, J., Gelman, A., Bolmgren, K., Allen, J. M., Travers, S. E., and Wolkovich, E. M.: Global
639 shifts in the phenological synchrony of species interactions over recent decades, *Proc. Natl. Acad. Sci. U. S. A.*,
640 115, 5211–5216, <https://doi.org/10.1073/pnas.1714511115>, 2018.

641 Kim, J., Seo, D., Jang, M., and Kim, J.: Augmentation of limited input data using an artificial neural network
642 method to improve the accuracy of water quality modeling in a large lake, *J. Hydrol.*, 602, 126817,
643 <https://doi.org/10.1016/j.jhydrol.2021.126817>, 2021.

644 Layden, A., Merchant, C., and Maccallum, S.: Global climatology of surface water temperatures of large lakes by
645 remote sensing, *Int. J. Climatol.*, 35, 4464–4479, <https://doi.org/10.1002/joc.4299>, 2015.

646 Lind, L., Eckstein, R. L., and Relyea, R. A.: Direct and indirect effects of climate change on distribution and
647 community composition of macrophytes in lentic systems, *Biol. Rev.*, 1686, 1677–1690,
648 <https://doi.org/10.1111/brv.12858>, 2022.

649 Lindenschmidt, K. E.: The effect of complexity on parameter sensitivity and model uncertainty in river water
650 quality modelling, *Ecol. Modell.*, 190, 72–86, <https://doi.org/10.1016/j.ecolmodel.2005.04.016>, 2006.

651 Mironov, D. V.: Parameterization of lakes in numerical weather prediction: Description of a lake model,
652 *Encyclopedic Dictionary of Archaeology*, Offenbach, Germany: DWD, 2008.

653 Nouchi, V., Kutser, T., Wüest, A., Müller, B., Odermatt, D., Baracchini, T., and Bouffard, D.: Resolving
654 biogeochemical processes in lakes using remote sensing, *Aquat. Sci.*, 81, 1–13, <https://doi.org/10.1007/s00027-019-0626-3>, 2019.

656 Nowlin, W. H., Davies, J. M., Nordin, R. N., and Mazumder, A.: Effects of water level fluctuation and short-term
657 climate variation on thermal and stratification regimes of a British Columbia reservoir and lake, *Lake Reserv.
658 Manag.*, 20, 91–109, <https://doi.org/10.1080/07438140409354354>, 2004.

659 Ottosson, F. and Abrahamsson, O.: Presentation and analysis of a model simulating epilimnetic and hypolimnetic
660 temperatures in lakes, *Ecol. Modell.*, 110, 233–253, [https://doi.org/10.1016/S0304-3800\(98\)00067-2](https://doi.org/10.1016/S0304-3800(98)00067-2), 1998.

661 Piccolroaz, S., Toffolon, M., and Majone, B.: A simple lumped model to convert air temperature into surface water
662 temperature in lakes, *Hydrol. Earth Syst. Sci.*, 17, 3323–3338, <https://doi.org/10.5194/hess-17-3323-2013>, 2013.

663 Piccolroaz, S., Woolway, R. I., and Merchant, C. J.: Global reconstruction of twentieth century lake surface water

- 664 temperature reveals different warming trends depending on the climatic zone, *Clim. Change*, 160, 427–442,
665 <https://doi.org/10.1007/s10584-020-02663-z>, 2020.
- 666 Poeter, E. P. and Hill, M. C.: Inverse models: A necessary next step in ground-water modeling, *Groundwater*, 35,
667 250–260, 1997.
- 668 Prats-Rodríguez, J. and Danis, P.-A.: inrae/ALAMODE-cuspy: cuspy v1.0,
669 <https://doi.org/10.5281/ZENODO.7585606>, 2023a.
- 670 Prats-Rodríguez, J. and Danis, P.-A.: inrae/ALAMODE-okp: okplm v1.0,
671 <https://doi.org/10.5281/ZENODO.7564750>, 2023b.
- 672 Prats, J. and Danis, P.-A.: Optimisation du réseau national de suivi pérenne in situ de la température des plans
673 d'eau : apport de la modélisation et des données satellitaires, [Rapport Rech. irstea, 93, <https://doi.org/hal-02602604>, 2015.
674
- 675 Prats, J. and Danis, P. A.: An epilimnion and hypolimnion temperature model based on air temperature and lake
676 characteristics, *Knowl. Manag. Aquat. Ecosyst.*, 8, <https://doi.org/10.1051/kmae/2019001>, 2019.
- 677 Prats, J., Reynaud, N., Rebière, D., Peroux, T., Tormos, T., and Danis, P. A.: LakeSST: Lake Skin Surface
678 Temperature in French inland water bodies for 1999-2016 from Landsat archives, *Earth Syst. Sci. Data*, 10, 727–
679 743, <https://doi.org/10.5194/essd-10-727-2018>, 2018.
- 680 Read, J. S., Winslow, L. A., Hansen, G. J. A., Van Den Hoek, J., Hanson, P. C., Bruce, L. C., and Markfort, C. D.:
681 Simulating 2368 temperate lakes reveals weak coherence in stratification phenology, *Ecol. Modell.*, 291, 142–150,
682 <https://doi.org/10.1016/j.ecolmodel.2014.07.029>, 2014.
- 683 Rimet, F., Anneville, O., Barbet, D., Chardon, C., Crépin, L., Domaizon, I., Dorioz, J. M., Espinat, L., Frossard,
684 V., Guillard, J., Goulon, C., Hamelet, V., Hustache, J. C., Jacquet, S., Lainé, L., Montuelle, B., Perney, P., Quetin,
685 P., Rasconi, S., Schellenberger, A., Tran-Khac, V., and Monet, G.: The Observatory on LAkes (OLA) database:
686 Sixty years of environmental data accessible to the public, *J. Limnol.*, 79, 164–178,
687 <https://doi.org/10.4081/jlimnol.2020.1944>, 2020.
- 688 Schaeffer, B. A., Iames, J., Dwyer, J., Urquhart, E., Salls, W., Rover, J., and Seegers, B.: An initial validation of
689 Landsat 5 and 7 derived surface water temperature for U.S. lakes, reservoirs, and estuaries, *Int. J. Remote Sens.*,
690 39, 7789–7805, <https://doi.org/10.1080/01431161.2018.1471545>, 2018.
- 691 Sharaf, N., Fadel, A., Bresciani, M., Giardino, C., Lemaire, B. J., Slim, K., Faour, G., and Vinçon-Leite, B.: Lake
692 surface temperature retrieval from Landsat-8 and retrospective analysis in Karaoun Reservoir, Lebanon, *J. Appl.*
693 *Remote Sens.*, 13, 1, <https://doi.org/10.1117/1.jrs.13.044505>, 2019.
- 694 Sharaf, N., Lemaire, B. J., Fadel, A., Slim, K., and Vinçon-Leite, B.: Assessing the thermal regime of poorly
695 monitored reservoirs with a combined satellite and three-dimensional modeling approach, *Int. Waters*, 11, 302–
696 314, <https://doi.org/10.1080/20442041.2021.1913937>, 2021.
- 697 Sharaf, N., Prats, J., Reynaud, N., Tormos, T., Peroux, T., and Danis, P. A.: LakeTSim (Lake Temperature
698 Simulations), *Rech. Data Gouv*, <https://doi.org/doi:10.57745/OF9WXR>, 2023.
- 699 Sharma, S., Walker, S. C., and Jackson, D. A.: Empirical modelling of lake water-temperature relationships: A
700 comparison of approaches, *Freshw. Biol.*, 53, 897–911, <https://doi.org/10.1111/j.1365-2427.2008.01943.x>, 2008.
- 701 Sharma, S., Gray, D. K., Read, J. S., O'Reilly, C. M., Schneider, P., Quadrat, A., Gries, C., Stefanoff, S., Hampton,
702 S. E., Hook, S., Lenters, J. D., Livingstone, D. M., McIntyre, P. B., Adrian, R., Allan, M. G., Anneville, O., Arvola,
703 L., Austin, J., Bailey, J., Baron, J. S., Brookes, J., Chen, Y., Daly, R., Dokulil, M., Dong, B., Ewing, K., De Eyto,
704 E., Hamilton, D., Havens, K., Haydon, S., Hetzenauer, H., Heneberry, J., Hetherington, A. L., Higgins, S. N.,
705 Hixson, E., Izmet'eva, L. R., Jones, B. M., Kangur, K., Kasprzak, P., Köster, O., Kraemer, B. M., Kumagai, M.,
706 Kuisisto, E., Leshkevich, G., May, L., MacIntyre, S., Müller-Navarra, D., Naumenko, M., Noges, P., Noges, T.,
707 Niederhauser, P., North, R. P., Paterson, A. M., Plisnier, P. D., Rigosi, A., Rimmer, A., Rogora, M., Rudstam, L.,
708 Rusak, J. A., Salmaso, N., Samal, N. R., Schindler, D. E., Schladow, G., Schmidt, S. R., Schultz, T., Silow, E. A.,
709 Straile, D., Teubner, K., Verburg, P., Voutilainen, A., Watkinson, A., Weyhenmeyer, G. A., Williamson, C. E.,
710 and Woo, K. H.: A global database of lake surface temperatures collected by in situ and satellite methods from
711 1985-2009, *Sci. Data*, 2, 1–19, <https://doi.org/10.1038/sdata.2015.8>, 2015.
- 712 Shatwell, T., Thiery, W., and Kirillin, G.: Future projections of temperature and mixing regime of European
713 temperate lakes, *Hydrol. Earth Syst. Sci.*, 23, 1533–1551, <https://doi.org/10.5194/hess-23-1533-2019>, 2019.

- 714 Snowling, S. D. and Kramer, J. R.: Evaluating modelling uncertainty for model selection, *Ecol. Modell.*, 138, 17–
715 30, [https://doi.org/10.1016/S0304-3800\(00\)00390-2](https://doi.org/10.1016/S0304-3800(00)00390-2), 2001.
- 716 Toffolon, M., Piccolroaz, S., Majone, B., Soja, A. M., Peeters, F., Schmid, M., and Wüest, A.: Prediction of surface
717 temperature in lakes with different morphology using air temperature, *Limnol. Oceanogr.*, 59, 2185–2202,
718 <https://doi.org/10.4319/lo.2014.59.6.2185>, 2014.
- 719 Vernay, M., Lafaysse, M., Mérindol, L., Giraud, G., and Morin, S.: Ensemble forecasting of snowpack conditions
720 and avalanche hazard, *Cold Reg. Sci. Technol.*, 120, 251–262, <https://doi.org/10.1016/j.coldregions.2015.04.010>,
721 2015.
- 722 Vernay, M., Lafaysse, M., Monteiro, D., Hagenmuller, P., Nheili, R., Samacoïts, R., Verfaillie, D., and Morin, S.:
723 The S2M meteorological and snow cover reanalysis over the French mountainous areas: description and evaluation
724 (1958-2021), *Earth Syst. Sci. Data*, 14, 1707–1733, <https://doi.org/10.5194/essd-14-1707-2022>, 2022.
- 725 White, J. T., Fienen, M. N., and Doherty, J. E.: A python framework for environmental model uncertainty analysis,
726 *Environ. Model. Softw.*, 85, 217–228, <https://doi.org/10.1016/j.envsoft.2016.08.017>, 2016.
- 727 White, J. T., Hunt, R. J., Fienen, M. N., Doherty, J. E., and Survey, U. S. G.: Approaches to highly parameterized
728 inversion: PEST++ Version 5, a software suite for parameter estimation, uncertainty analysis, management
729 optimization and sensitivity analysis:, *U.S. Geological Survey Techniques and Methods 7C26*, 52 pp.,
730 <https://doi.org/10.3133/tm7C26>, 2020.
- 731 Woolway, R. I. and Merchant, C. J.: Worldwide alteration of lake mixing regimes in response to climate change,
732 *Nat. Geosci.*, 12, 271–276, <https://doi.org/10.1038/s41561-019-0322-x>, 2019.
- 733 Woolway, R. I., Sharma, S., and Smol, J. P.: Lakes in Hot Water : The Impacts of a Changing Climate on Aquatic
734 Ecosystems, *Bioscience*, <https://doi.org/10.1093/biosci/biac052>, 2022.
- 735 Yang, K., Yu, Z., Luo, Y., Yang, Y., Zhao, L., and Zhou, X.: Spatial and temporal variations in the relationship
736 between lake water surface temperatures and water quality - A case study of Dianchi Lake, *Sci. Total Environ.*,
737 624, 859–871, <https://doi.org/10.1016/j.scitotenv.2017.12.119>, 2018.
- 738 Yang, K., Yu, Z., and Luo, Y.: Analysis on driving factors of lake surface water temperature for major lakes in
739 Yunnan-Guizhou Plateau, *Water Res.*, 184, 116018, <https://doi.org/10.1016/j.watres.2020.116018>, 2020.
- 740